Interstitial Lung Diseases

Christina Mueller-Mang, Helmut Ringl,
and Christian Herold

Contents

C. Mueller-Mang (✉) • H. Ringl • C. Herold
Department of Biomedical Imaging and Image-guided Therapy, Medical University of Vienna, Währinger Gürtel 18-20, A-1090 Vienna, Austria
e-mail: mueller-mang@ct-mrt.com

Key Points

The term interstitial lung diseases (ILD) comprises a diverse group of diseases that lead to *inflammation* and *fibrosis* of the alveoli, distal airways, and septal interstitium of the lungs. The ILD consist of disorders of *known cause* (e.g., collagen vascular diseases, drug-related diseases) as well as disorders of unknown etiology. The latter include *idiopathic interstitial pneumonias* (IIPs), and a group of miscellaneous, rare, but nonetheless interesting, diseases. In patients with ILD, MDCT enriches the diagnostic armamentarium by allowing volumetric high-resolution scanning, i.e., continuous data acquisition with thin collimation and a high spatial frequency reconstruction algorithm. *CT* is a key method in the identification and management of patients with ILD. It not only improves the detection and characterization of parenchymal abnormalities, but also increases the accuracy of diagnosis. The spectrum of morphologic characteristics that are indicative of interstitial lung disease is relatively limited and includes the linear and reticular pattern, the nodular pattern, the increased attenuation pattern (such as ground-glass opacities and consolidation), and the low attenuation pattern (such as emphysema and cystic lung diseases). In the correct clinical context, some *patterns* or combination of patterns, together with the *anatomic distribution* of the abnormality, i.e., from the lung apex to the base, or peripheral subpleural versus central bronchovascular, can lead the interpreter to a specific diagnosis. However, due

Med Radiol Diagn Imaging (2017)
DOI 10.1007/174_2017_151, © Springer International Publishing AG

to an overlap of the CT morphology between the various entities, the final diagnosis of many ILD requires close cooperation between clinicians and radiologists and complementary *lung biopsy* is recommended in many cases.

1 Introduction

The interstitial lung diseases (ILD) are a heterogeneous group of lung disorders that result from damage to the lung by various forms of inflammation and fibrosis. By definition, ILDs involve the lung interstitium that forms a fibrous skeleton for the lungs. However, many of the conditions that have been traditionally included under the heading of ILDs are actually associated with extensive alterations of the alveolar and airway architecture. For this reason, the terms "diffuse infiltrative lung disease" or "diffuse parenchymal lung disease" are preferable. Still, the term ILDs remains in common clinical usage.

ILD represent more than 200 different entities, and various and often confusing classification systems are simultaneously used. One useful approach to classification is to separate the ILD into diseases of known and unknown etiology (Table 1). ILD of unknown etiology (65% of all ILD) can be further subdivided into the group of idiopathic interstitial pneumonias (IIP), and a group comprising several rare but nevertheless interesting diseases with distinctive clinicopathologic features, such as lymphangioleiomyomatosis, Langerhans cell histiocytosis, pulmonary alveolar proteinosis, and pulmonary alveolar microlithiasis. Sarcoidosis has an exceptional position within the group of ILDs of unknown cause, as it is relatively common and can present as a systemic disease.

CT scanning is the most important noninvasive diagnostic key to the identification and characterization of ILD, and aids the radiologist and the clinician in the management of patients who carry this disorder. Among all noninvasive methods, it provides the highest sensitivity and specificity in the detection of

Table 1 Classification of interstitial lung diseases (ILDs)

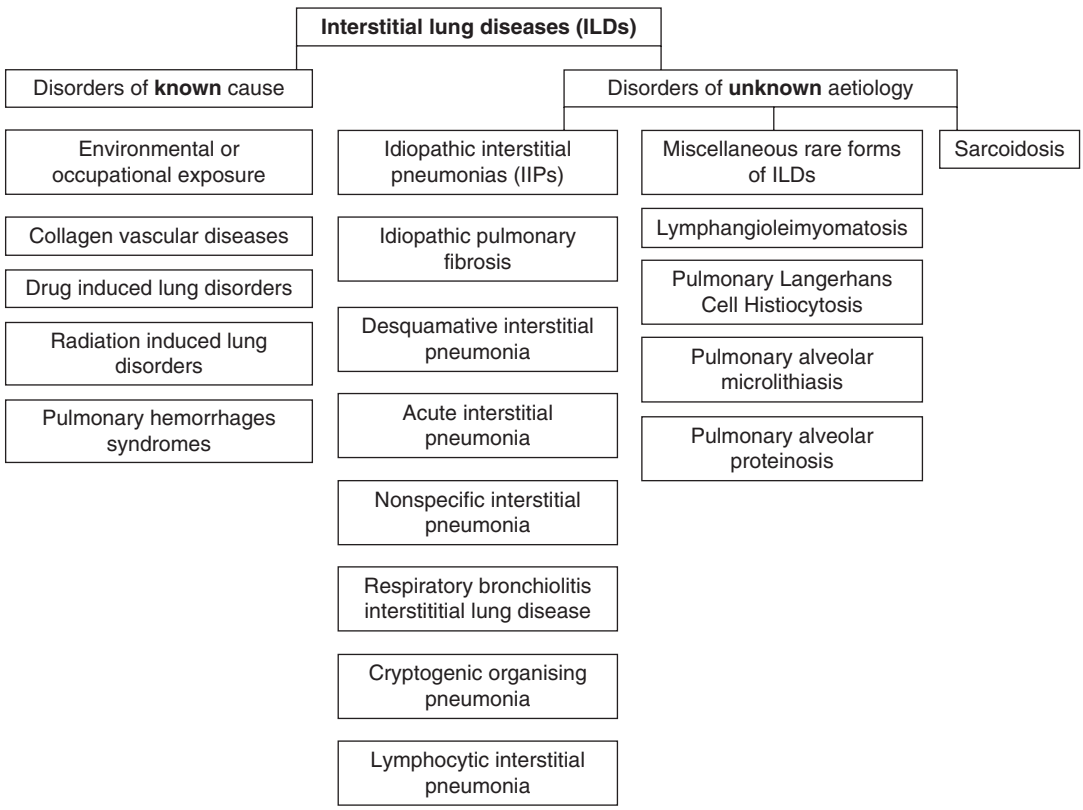

ILD. Also, it has a higher accuracy in comparison to the clinical assessment, lung function tests and chest radiography in diagnosing a specific disorder, and adds diagnostic accuracy and confidence when added to the clinical assessment and the chest radiogram. Finally, CT helps to identify the best location for lung biopsy, and provides an important basis for the follow-up of ILD patients.

2 Anatomic and Technical Considerations

2.1 Normal Lung Anatomy

The correct interpretation of ILD requires a fundamental understanding of normal lung anatomy. The identification of the patterns of infiltration and distribution is a key to the establishment of a correct list of differential diagnoses, and sometimes to the diagnosis itself. In this sense, HRCT provides an insight into lung morphology and architecture, comparable to or even beyond macroscopic pathology. The following anatomic structures and architectural components need to be considered:

2.1.1 The Peribronchovascular Interstitium

The peribronchovascular interstitium is also known as the axial interstitium and runs along the pulmonary arteries, the bronchial branches, and the lymphatics from the hilar regions to the lung periphery. It is not visible in healthy individuals but lymphatic diseases, such as sarcoidosis, lymphangitic carcinomatosis or pulmonary edema can lead to smooth, nodular or irregular thickening of the peribronchovascular interstitium.

2.1.2 The Secondary Pulmonary Lobule

The secondary pulmonary lobule (SPL) is the smallest anatomical unit of the lungs that can be identified on HRCT scans (Fig. 1). Whereas in normal lungs, these polyhedral structures are only allusively visible in the anterior and lateral portions of the pulmonary parenchyma, they may be clearly identifiable in any region when ILD are present.

Typical SPLs are irregular polyhedral units which vary in size, measuring from approximately 1–2.5 cm in diameter and incorporating up to 24 acini (Webb 2006). An average diameter

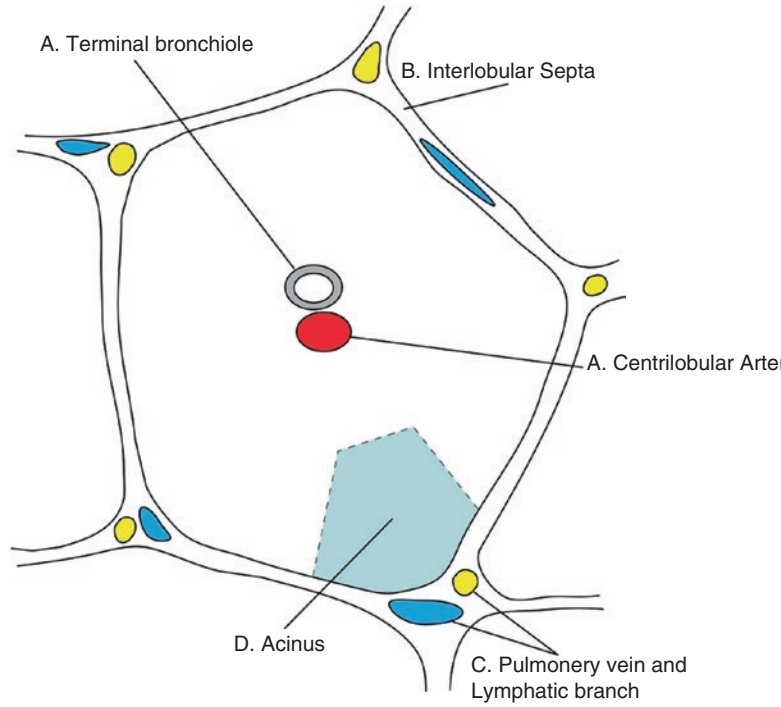

Fig. 1 Secondary pulmonary lobule (*A*: Centrilobular arteries and bronchioles with a diameter of approximately 1 mm; *B*: Interlobular septa with a thickness of approximately 0.1 mm; *C*: Pulmonary vein and lymphatic branch with diameters of 0.5 mm each; *D*: Acinus—never visible on CT scans)

for SPLs ranges from 11 to 17 mm in adults. The SPL is surrounded by a mantle of connective tissue septa. A central bronchovascular bundle, consisting of the lobular bronchiole and the accompanying pulmonary artery, enters the center of the SPL, where the bronchiole bifurcates into three to five terminal bronchioles. The region near the origin of the terminal bronchioles is termed the "centrilobular" region. Thus, on thin-section CT images, the secondary pulmonary lobule can be divided into three components: the interlobular septa; the centrilobular region; and the lobular parenchyma.

2.1.3 Interlobular Septa

The interlobular septa extend from the pleural surface of the lung inward, and surround the SPL. They consist of connective tissue, house pulmonary veins, and lymphatics and belong to the peripheral interstitial fiber system (Weibel 1979). Interlobular septa are well developed in the periphery of the lungs, and in particular in the lung apex, and near the anterior, lower, mediastinal, and diaphragmatic surfaces. They are key structures to the identification of pulmonary involvement in ILD, because disorders such as interstitial lung edema, sarcoidosis, or lymphangitic carcinomatosis commonly lead to thickening and consequently to better visibility of these structures.

2.1.4 Centrilobular Region

The centrilobular region contains the pulmonary artery and bronchiolar branches that supply the lobule. Because lobules do not arise at a specific branching generation of the bronchial or arterial tree, it is difficult to impossible to define exactly which specific bronchus or artery supplies that secondary lobule. However, lobular bronchioles are rarely seen in normal individuals since their lumen measures approximately 1 mm in diameter, and their wall 0.15 mm, respectively. Likewise, the more peripheral terminal and respiratory bronchioles cannot be resolved at CT (Murata et al. 1986). It is only in diseases of the small airways that abnormal bronchi can be visualized through thickened walls, peribronchiolar inflammation, and/or intrabronchiolar fluid and mucus accumulations. Centrilobular arteries can be depicted at CT scans of normal and diseased individuals. Because of the anatomic properties of the lungs, centrilobular abnormalities are best seen in the lung periphery and near the hila. The centrilobular region can be affected by vascular and small airway diseases.

2.1.5 Lobular Parenchyma

The lobular parenchyma consists of alveoli, the associated pulmonary capillary bed, and a fine network of connective tissue which has been termed the *intralobular interstitium*. These structures are too small to be directly visualized on thin-section CT, but may be indirectly assessed as they are responsible for the background density of the lung on CT scans. Parenchymal background density reflects the proportions of fluid (blood and extravascular fluid), gas, and tissue. When ILD causes an increase of fluid or cells within the alveoli, or thickening of the alveolar septa through cellular infiltration or fibrosis, then parenchymal background density will change in turn and ground-glass opacities may be identified at CT. Conversely, a decrease in fluid, cells, and tissue (in relation to air), as seen in emphysema, causes a reduction of the parenchymal density, in comparison to the normal state. The thickening of the intralobular interstitium and the interlobular septa by fibrosis or infiltration leads to a reticular pattern.

2.2 CT-Technique

For patients with ILD, the detailed visualization of the lung parenchyma and the depiction of the smallest abnormal finding is of paramount importance for any imaging approach. In order to achieve highest possible spatial resolution, a thin acquisition section thickness, a high spatial frequency reconstruction algorithm, a certain amount of radiation dose, and a small field of view are mandatory.

2.2.1 Spaced High-Resolution CT

For decades, patients with ILD have traditionally been assessed with HRCT (Mayo et al. 1987). This technique uses a "step-and-shoot" or "spaced" approach, in which thin sections with

0.5–1.5 mm thickness scans are obtained at 10–20 mm intervals. The large gaps between the sections considerably lower the radiation dose applied and allows for increasing the dose for each of the thin sections. Therefore, each of these sections offers a very good image quality with low noise and high spatial resolution. This high quality comes along with the disadvantage of a discontinuous CT data set with 10–20 mm gaps between the sections hampering the ability for exact comparison to prior examinations if the images are not perfectly aligned in z-direction. This "classic" HRCT technique still plays a decisive role in the noninvasive investigation of patients with pulmonary disease of a diffuse distribution pattern (Hansell 2001).

2.2.2 Volumetric High-Resolution CT

With the advent of MDCT, volumetric high-resolution imaging has become feasible and allows for imaging of the entire lung with high spatial resolution and the generation of a continuous dataset without gaps. In addition to visualize diffuse structural changes of the lung parenchyma it adds the ability to detect and interpret sparsely distributed abnormalities of the lung parenchyma as well as focal disease which might have been missed using the classic spaced HRCT approach due to the gaps between the sections. The resulting volumetric, near isotropic data sets also permit the reconstruction of high quality multiplanar images which enable for better recognition of the distribution of disease, for example, to identify and rate a possible apico-basal gradient in the lung. Finally, continuous data acquisition allows the generation of thick maximum intensity projections (MIP) which are helpful for the detection of micronodular disease and centrilobular abnormalities.

There are also some trade-offs with volumetric high-resolution CT scanning. For most scanners, except the most recent generation, the radiation dose is five to ten times higher, and the image quality concerning noise and spatial in-plane resolution is lower in comparison to the introduced sequential HRCT. This image quality reduction is most apparent in the depiction of small septa, ground-glass opacities as well in increased image noise (Studler et al. 2005). Its clinical significance has yet to be determined.

2.2.3 Other Parameters Influencing Radiation Dose

Over the last few years most vendors significantly improved their CT detector and reconstruction technology. Detector quantum efficiency as well as local electronic processing and data transfer have been considerable increased allowing for better image quality compared to last detector generation or lower dose for the same image quality that was reached a few years ago.

2.2.4 Reconstruction Kernels

Filtered back-projection (FBP) has been the standard reconstruction method over decades for all CT protocols. However, in the last years, for most of the regions of the body, the recent generations of iterative reconstruction kernels have become standard of care and outperformed FBP in terms of image quality. However, due to the requirements in terms of spatial resolution for visualizing the lung accurately, there is still a controversy in radiology, whether iterative reconstruction should be used for the lung and which strength and software algorithm is best suited. Therefore, the iterative reconstruction algorithm should carefully be selected and should be applied only with moderate strength for adequate visualization of the lung parenchyma.

2.2.5 Tube Voltage Selection and Tube Current Modulation

Using lower tube voltages can considerable contribute to saving radiation dose. Lowering this parameter is however limited due to patient size and the ability of the X-ray tube used to compensate with higher tube currents. This can be done manually or automatically with a built-in tube voltage selection. To end up with the right number of photons, CT scanners also offer an automatic tube current modulation.

These techniques allow for autoregulation of the two most important parameters of the X-Ray tube. They compute the optimum photon energy depending on the size of the patient as well as the tube current necessary based on a given quality factor or reference mAs of the protocol. These two techniques should always be enabled for best quality at the lowest achievable dose (Prosch et al. 2013).

2.2.6 Spectral Shaping

In addition to these improvements, spectral shaping has been introduced as an additional dose saving technique (Gordic et al. 2014). It consists basically of a tin filter, that absorbs photons at lower energy levels before they leave the X-ray tube. This technique can be applied at tube voltages at 100 kVp or above and allows for additional dose savings as well as for reduction of beam hardening artifacts. However, it is not suitable for iodine contrast enhanced scans, because higher energy photons show less absorption by iodine then low energy photons.

2.2.7 Low Dose CT

Depending on the device used, volumetric spiral CT of the lung can be performed with dose values quite below the national reference values, if new detectors, low tube voltages or spectral shaping are applied. However, application of dedicated low dose CT has to be carried out with great care if it comes to patients with ILD. Whereas it is perfectly feasible to use ultralow dose for the follow-up exam of lung nodules, because nodules above 4 mm can be accurately visualized with a low number of photons, this does not apply for small septa, very small nodules and ground-glass opacities. These structures may be over- or underestimated in the low dose CT (Lim et al. 2016).

2.2.8 Protocol Decision

The lack of a standard and the number of different scanners with different aged technology in operation in clinical routine result in various CT protocols used for imaging ILD (Prosch et al. 2013).

The question whether a spaced HRCT or a volumetric approach should be performed might be answered by the scanner generation and the corresponding dose efficiency of the device. As a decision support, the reference values for CT of the lung of the applicable country can be used. If a volumetric HRCT (section thickness < 1.5 mm) with sufficient image quality on the particular device produces more than, e.g., between 250 and 350 DLP, than a spaced HRCT might be used instead. However, nowadays the vast majority of specialized lung radiologist recommend volumetric HRCT, if an adequate scanner is available.

Therefore, whenever a modern CT is available the suitable CT protocol for diagnosis of possible ILD should offer a volumetric dataset with the following parameters: section thickness (ST) ≤ 1.5 mm, RI slightly thinner than ST (RI = ST*0.7), a high spatial frequency reconstruction algorithm (FBP or iterative moderate strength), DLP ≤ the national reference value for thoracic CT (e.g., ≤ 300 mGy/cm), Tube current: reference mAs or quality factor highly dependent on the device, automatic kVp selection enabled, dose modulation enabled. Low dose and ultra low dose scans should be avoided for the primary assessment. For most cases, no iodine contrast is needed.

3 HRCT Pattern

3.1 Linear and Reticular Pattern

The linear pattern is characterized by interlobular septal thickening and outlines the usually hardly perceptible polygonal structure of the secondary pulmonary lobule. Centrally, a dot-like structure is usually visible representing the centrilobular artery. The interlobular septal thickening can be smooth, like in interstitial lung edema (Fig. 2) whereas nodular interlobular septal thickening is most commonly seen in patients with sarcoidosis. In lymphangitis carcinomatosis interlobular septal thickening can be either smooth or nodular and is frequently unilateral or focal as opposed to bilateral lung involvement in interstitial edema. Irregular interlobular septal thickening is typically seen in fibrotic lung disease and is usually associated with thickening of the fine interstitial network within the secondary pulmonary lobule, the so-called intralobular septa. The combination of interlobular and intralobular septal thickening represents the reticular pattern. Additional signs of lung fibrosis include traction bronchiectasis and honeycombing.

3.2 Nodular Pattern

Nodular lung diseases present with multiple nodules smaller than 1 cm. According to the distribution of these nodules in relation to the secondary pulmonary lobules three nodular patterns can be distinguished on HRCT: (1) perilymphatic, (2) centrilobular, and (3) random.

3.2.1 Perilymphatic Nodules

Perilymphatic nodules are distributed along the pulmonary lymphatic spaces that are predominantly found in four locations: the parahilar and the centrilobular peribronchovascular interstitium, the subpleural interstitium, and the interlobular septa. Perilymphatic nodules are typically well defined and most commonly encountered in sarcoidosis, silicosis, and lymphangiosis carcinomatosa (Fig. 3a).

Fig. 2 HRCT shows smooth interlobular septal thickening with outlining of the secondary pulmonary lobule in interstitial lung edema

3.2.2 Centrilobular Nodules

Centrilobular nodules are located in the center of the secondary pulmonary lobule next to the centrilobular peribronchovascular structures and thus can be due to vascular, lymphatic or small airway diseases, the latter being the most common cause. In centrilobular diseases the subpleural interstitium and the fissures are typically spared. Centrilobular nodules can either present with ground-glass opacity or homogeneous soft tissue attenuation. Ground-glass opacity nodules tend to be ill-defined and are most commonly seen in the subacute stage of hypersensitivity pneumonitis (HP) and in respiratory bronchiolitis (RB) (Fig. 3b). Other less frequent causes include Langerhans cell histiocytosis, pulmonary edema, and pulmonary hemorrhage. Soft attenuation centrilobular nodules tend to have an asymmetric distribution and can progress to patchy consolidations.

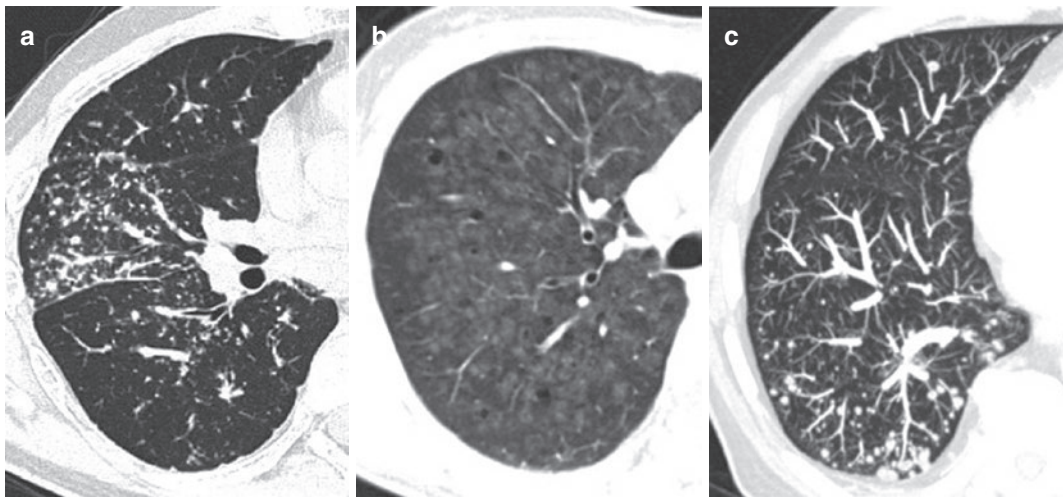

Fig. 3 (**a**–**c**) Perilymphatic nodules: Well defined nodules are seen in the peribronchovascular, subpleural, centrilobular, and interlobular interstitium in a patient with sarcoidosis (**a**). Centrilobular nodules: Multiple centrilobular nodules of ground-glass opacity can be found in a patient with hypersensitivity pneumonitis (**b**). (**c**) Random nodules: multiple, diffusely distributed nodules of various size and with involvement of the pleural surface can be seen on this MIP CT image in a patient with haematogenous metastases (**c**)

They are associated with endobronchial spread of disease, such as in bronchopneumonia, aspiration, and invasive mucinous adenocarcinoma.

The tree-in-bud pattern is a subtype of a centrilobular pattern and characterized by multiple nodules that show a linear and branching distribution, resembling a budding tree. The pattern is caused by dilatation and impaction of the centrilobular bronchioles with mucus, pus, or blood. The tree-in-bud pattern is almost always caused by infection, most commonly due to bacteria or mycobacteria. In chronic disease, bronchiectasis and bronchial wall thickening may be present. Extensive and diffuse tree-in-bud pattern is typically for Kartagener's syndrome and cystic fibrosis.

3.2.3 Random Nodules

Random nodules are usually sharply marginated and of soft tissue attenuation. They show a diffuse distribution with involvement of the pleural surfaces. They are caused by hematogenous dissemination and are most commonly due to metastatic disease (Fig. 3c). They may show a basilar dominance in size and number. The differential diagnosis includes miliary tuberculosis and miliary fungal infection.

3.3 High Attenuation Pattern

The lung density can be increased by either ground-glass opacity or consolidation. Ground-glass opacity leads to a hazy increase of lung density without obscuring the lung vessels. In consolidation the lung density is homogenously increased and the vessels are no longer visible. Ground-glass opacity is a common but nonspecific pattern. In the acute clinical setting it is frequently associated with infectious diseases, pulmonary edema, and hemorrhage. It can also be the main imaging finding in acute hypersensitivity pneumonitis and acute eosinophilic pneumonia. In patients with chronic symptoms ground-glass opacity is typically seen in various subtypes of interstitial pneumonia.

The combination of ground-glass opacity and consolidation is common and suggestive of organizing pneumonia, chronic eosinophilic pneumonia, and ARDS. Less common, but nevertheless important causes of combined ground-glass opacity and consolidation are invasive adenocarcinoma and intrapulmonary lymphoma (Fig. 4).

The crazy paving pattern is a term reserved for ground-glass opacities with superimposed thickening of the interlobular and intralobular septa. It has been initially described in patients with alveolar proteinosis, but is nonspecific and may be seen in infectious, neoplastic, inhalative, and hemorrhagic lung diseases.The mosaic attenuation pattern is characterized by the presence of sharply demarcated areas of various lung density. In several ILDs, notably in NSIP, the heterogeneous lung attenuation is due to patchy ground-glass opacities next to normal lung parenchyma. In this setting, areas of higher attenuation represent the interstitial process and areas of lower attenuation represent the normal lung parenchyma. Other causes of mosaic attenuation pattern are obliterative small-airways disease or occlusive vascular disease. In small airway disease bronchiolar obstruction leads air trapping, a phenomenon that is characterized by focal zones of decreased attenuation and can be enhanced by expiratory scans. It is typically seen in bronchiolitis obliterans syndrome due to chronic lung transplant rejection or infection.

Fig. 4 Multifocal adenocarcinoma of the lung presenting as patchy consolidations and ground-glass opacities. In addition, bilateral pleural effusions can be seen

Mosaic attenuation pattern due to vascular disease is referred to as mosaic perfusion and is most commonly seen in chronic thromboembolic pulmonary hypertension (CTEPH). Due to the regional decrease in lung perfusion, the abnormal lung is lucent and vessels appear smaller in comparison to vessels in the normal lung.

A mosaic attenuation pattern that is caused by a combination of ground-glass opacities and mosaic perfusion/air trapping has been termed the headcheese sign and is most commonly found in subacute hypersensitivity pneumonitis.

3.4 Low Attenuation Pattern

The low attenuation pattern can be seen in cysts, emphysema, and honeycombing. Lung cysts have a thin wall and are typically greater than 1 cm in size. They can be occasionally found in patients who are otherwise normal but the presence of more than a few cysts suggests a cystic lung disease, such as lymphangioleiomyomatosis, Langerhans cell histiocytosis, and lymphoid interstitial pneumonia. Postinfectious pneumatoceles from pneumocystis pneumonia can also present as cystic lung disease.

Depending on the area of lung destruction with regard to the secondary pulmonary lobule, emphysema can be subdivided in centrilobular, panlobular, and paraseptal. As opposed to true cysts, the lucencies in centrilobular and panlobular emphysema do not have a wall. However, perifocal fibrosis or atelectasis may simulate a wall in some emphysematous regions. In addition, in paraseptal empyshema, the supleural areas of emphysema are outlined by a discrete and thin wall that corresponds to the interlobular septa.

Honeycombing is a typical sign of advanced fibrosis and the most important HRCT feature of usual interstitial pneumonia (UIP). It is characterized by multiple layers of subpleural cysts with a defined wall (1–3 mm) and a diameter between 3 and 10 mm. In UIP honeycombing is predominantly found in the basal zones of both lungs, whereas in end stage fibrosis due to hypersensitivity pneumonitis, sarcoidosis or collagen vascular diseases honeycombing tends to dominate in the apical or central zones of the lung (Fig. 5a–c). As the presence of honeycombing reflects advanced fibrosis it is important to avoid pitfalls such as traction bronchiectasis, subpleural emphysema, or cystic lung diseases.

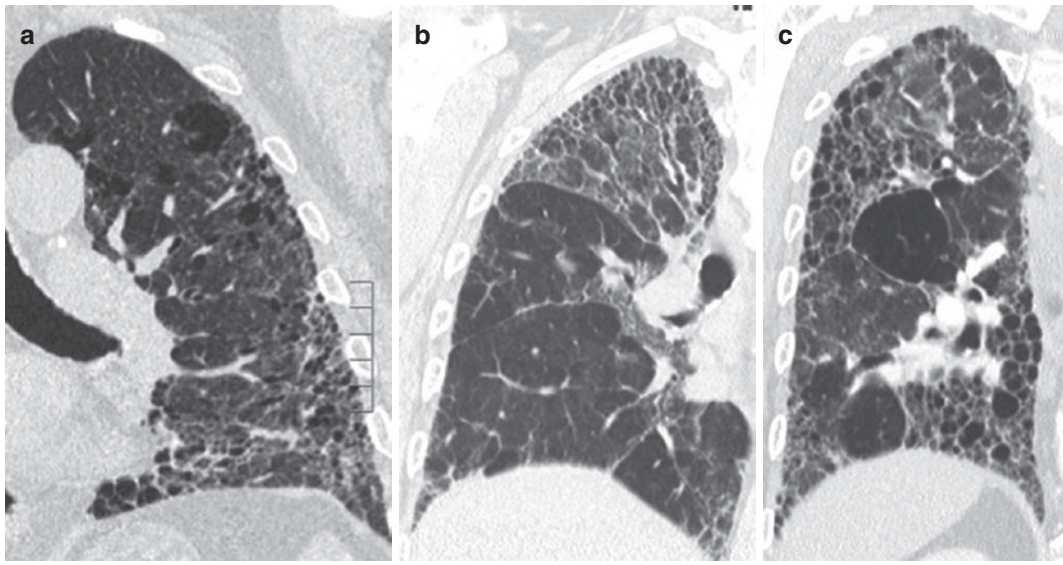

Fig. 5 (**a**–**c**) Honeycombing in UIP presenting as multiple layers of cysts in a basal and peripheral distribution (**a**). Honeycombing in hypersensitivity pneumonitis with involvement of the right upper lobe only (**b**). Honeycombing in sarcoidosis with cystic lesions throughout the entire lung (**c**)

4 Interstitial Lung Diseases That Have No Known Cause

In many ILDs, the etiology remains unknown. Most are uncommon, and some, such as alveolar microlithiasis, are exceedingly rare, but others, such as idiopathic pulmonary fibrosis and sarcoidosis, are quite common.

4.1 Idiopathic Interstitial Pneumonias (IIP)

The term idiopathic interstitial pneumonias refers to a group of seven entities with distinct histologic patterns: idiopathic pulmonary fibrosis (IPF), characterized by the pattern of usual interstitial pneumonia (UIP); nonspecific interstitial pneumonia (NSIP); cryptogenic organizing pneumonia (COP); respiratory bronchiolitis-associated interstitial lung disease (RB-ILD); desquamative interstitial pneumonia (DIP); lymphoid interstitial pneumonia (LIP); and acute interstitial pneumonia (AIP).

In their idiopathic form, IIPs are rare diseases. They are, nevertheless, considered prototypes of more common secondary interstitial lung disorders, such as sarcoidosis, vasculitis, and connective tissue diseases, although they appear to follow a different and often less aggressive clinical course. The advent of HRCT has had a profound impact on the imaging of IIPs, because the detailed delineation of the lung anatomy allows a close correlation between the histologic patterns of IIPs and the CT features. On the basis of CT morphology and in the correct clinical context, the radiologist can achieve an accurate diagnosis in many cases. However, due to overlap between the various entities, complementary lung biopsy is recommended in cases with indistinct imaging findings.

4.1.1 Idiopathic Pulmonary Fibrosis (IPF)

IPF is by far the most common IIP (approximately 50% of IIP), and has a substantially poorer long-term survival rate than the other IIPs (median survival, 2–5 years) (Katzenstein and Myers 1998). IPF shares nonspecific clinical symptoms, such as gradual onset of progressive dyspnea and cough, with other IIP. There is a slight male predominance and patients are usually over the age of 50. Typically, patients do not respond to corticosteroid treatment. In 2014 two antifibrotic drugs, nintedanib and pirfenidone were approved for treatment of IPF but survival benefit has not been established with either agent (Antoniou et al. 2016). Therefore currently, the only life-prolonging therapy consists of lung transplantation (Thabut et al. 2003).

While the term IPF characterizes the clinical entity, the term "usual interstitial pneumonia" is used to describe the histologic and radiologic patterns associated with IPF. The histologic and radiologic features of UIP are characterized by heterogeneity with areas of normal lung alternating with patchy fibrosis. The typical computed tomographic (CT) findings in UIP are predominantly basal and peripheral reticular opacities with honeycombing and traction bronchiectasis (Fig. 6a) (Mueller-Mang et al. 2007). Ground-glass opacities are usually present, but limited in extent. According to the recent guidelines established by American, European, Japanese and Latin American Societies radiologist should use the following terms to indicate the diagnostic confidence of a UIP pattern (Raghu et al. 2011): (definite) "UIP" pattern, "possible UIP" pattern, "inconsistent with UIP" pattern. A pattern of "UIP" requires the presence of following four CT findings: (1) subpleural, basal predominance, (2) reticular opacities, (3) honeycombing with or without traction bronchiectasis, and (4) absence of features listed as inconsistent with UIP pattern. A "possible UIP" pattern is defined by the same criteria as "UIP" pattern but without honeycombing. HRCT findings that are "inconsistent with UIP" include (1) an upper or mid-lung predominance, (2) a peribronchovascular predominance, (3) extensive ground-glass opacities, exceeding reticulation in extent, (4) profuse micronodules (bilateral, predominantly upper lobes), (5) discrete cysts, (6) diffuse mosaic attenuation or air trapping, (7) segmental or lobar consolidation and are listed in detail in Table 2.

Patients with IPF may present with rapid respiratory worsening during the course of their disease. When a cause, such as pulmonary embolism, pneumothorax, or cardiac failure, cannot be

defined this is termed acute exacerbation of IPF. On HRCT widespread diffuse or patchy ground-glass opacities have been observed in these patients, correlating to diffuse alveolar damage (DAD) on histopathology (Fig. 6b) (Kim et al. 2006). Other complications that should be noted in patients with IPF include opportunistic pulmonary infections (e.g., Pneumocystis Jiroveci), pulmonary hypertension, and an increased risk of bronchial carcinoma (Bouros et al. 2002). Therefore, CT scanning should involve a combination of standard volumetric CT with sequential HRCT.

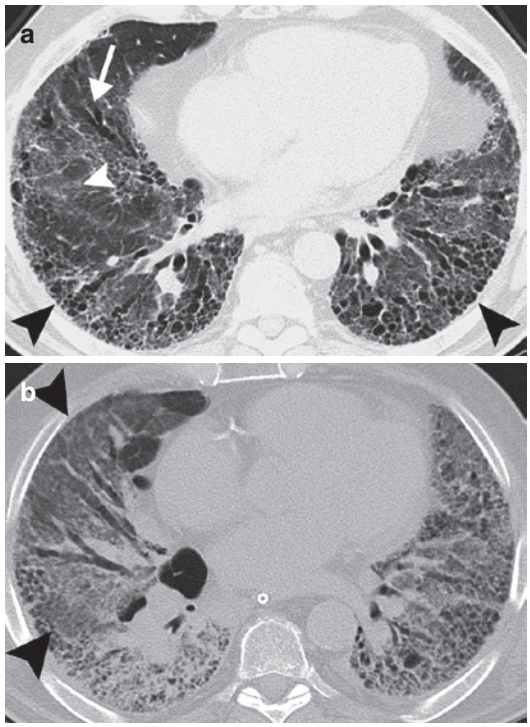

Fig. 6 (**a**, **b**) Axial CT image in a 63-year-old man with usual interstitial pneumonia (UIP)/idiopathic pulmonary fibrosis (IPF) shows bilateral reticular opacities, honeycombing (*black arrowheads*), and traction bronchiectasis (*arrow*). In addition, patchy ground-glass opacities are present (*white arrowheads*) (**a**). Acute exacerbation in the same patient shows marked progression of ground-glass opacities *(arrowheads*) (**b**)

4.1.2 Nonspecific Interstitial Pneumonia (NSIP)

Given the clinical, radiologic, and pathologic variability of NSIP, the diagnostic approach to this entity is challenging. Patients with NSIP are usually between 40 and 50 years old, and men and women are equally affected. Compared to IPF, patients with NSIP have a variable, but overall more favorable, course of disease and the majority of patients stabilize or improve on corticosteroid therapy. According to the predominance of either inflammatory cells or fibrosis, NSIP is histologically subdivided into a cellular and a fibrotic subtype. Cellular NSIP is less common than fibrotic NSIP and carries a substantially better prognosis (Travis et al. 2000). On HRCT, NSIP is characterized by patchy ground-glass opacities combined with irregular linear or reticular opacities (Johkoh et al. 2002) (Fig. 7a, b). In fibrotic NSIP traction bronchiectasis become more evident and honeycombing may be present, but is typically limited in severity and extent. It has also been referred to as microcystic honeycombing (Desai et al. 2004). In contrast to the heterogeneous lung involvement and the typical

Table 2 ATS/ERS/JRS/ALAT criteria for HRCT diagnosis of usual interstitial pneumonia (Raghu et al. 2011)

UIP pattern (all four features)	Possible UIP pattern (all three features)	Inconsistent with UIP pattern
Subpleural, basal predominance	Subpleural, basal predominance	Upper or mid-lung predominance
Reticular opacities	Reticular opacities	Peribronchovascular predominance
Honeycombing with or without traction bronchiectasis	Absence of features listed as "inconsistent" with UIP pattern	Extensive ground-glass opacities (extent > reticular abnormality)
Absence of features listed as "inconsistent" with UIP pattern		Profuse micronodules (bilateral, predominantly upper lobes)
		Discrete cysts multiple, bilateral, away from areas of honeycombing
		Diffuse mosaic attenuation or air trapping (bilateral in three or more lobes)
		Segmental or lobular consolidation

apico-basal gradient in UIP, HRCT in NSIP reveals rather symmetric and homogeneous lung involvement without an obvious gradient (Fig. 8). The relative sparing of the immediate subpleural space is highly predictive of NSIP and present in 20–50% of cases (Fig. 9).

4.1.3 Cryptogenic Organizing Pneumonia (COP)

COP was formerly referred to as "bronchiolitis obliterans organizing pneumonia (BOOP)" and is characterized by the histologic pattern of organizing pneumonia (OP). There is no gender predilection. Patients usually present between 50 and 60 years of age, and typically report a respiratory tract infection preceding their symptoms. In its idiopathic form (as COP), OP is rare; however, it is frequently encountered in association with collagen vascular diseases, and in infectious and drug-induced lung diseases (Cordier 2000). On corticosteroid therapy, patient usually experience complete recovery, but relapses are common. The histologic hallmark of COP is the development of granulation tissue polyps within the alveolar ducts

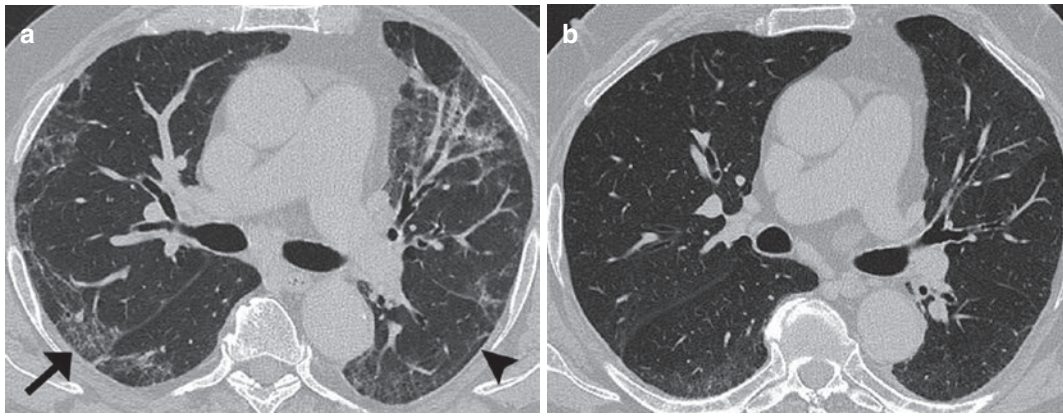

Fig. 7 (**a**, **b**) Axial CT image in a 61-year-old man with NSIP shows bilateral subpleural irregular linear opacities (*arrowhead*) and ground-glass opacities (*arrow*) (**a**). Follow-up CT image obtained after 6 months of corticosteroid therapy shows improvement, with partial resolution of the linear opacities and ground-glass opacities (**b**)

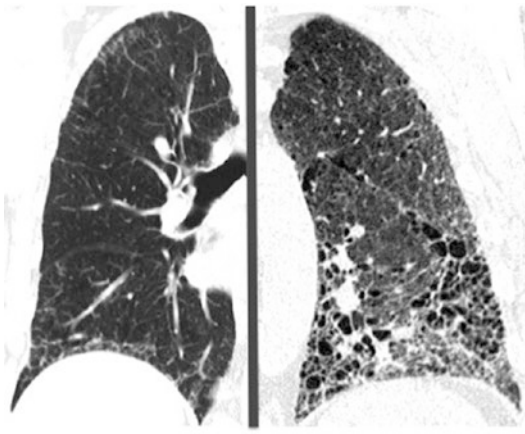

Fig. 8 Comparison of CT features between NSIP and UIP. NSIP (*left*) shows diffuse lung involvement with bilateral, peripherally located linear and reticular opacities. In UIP (*right*) the lung abnormalities show a typical apico-basal gradient with predominance of honeycombing

Fig. 9 HRCT shows characteristic subpleural sparing of reticular opacities (*arrows*) in a 67-year-old patient with NSIP

and alveoli, with preservation of the lung architecture. On HRCT, COP is characterized by patchy peripheral or peribronchial consolidations that resemble pneumonic infiltrates and predominate in the lower lung lobes (Lee et al. 1994) (Fig. 10a, b). Frequently, air bronchograms and perifocal ground-glass opacities can be found. Other common findings include sparing of the outermost subpleural area and mild cylindrical bronchiectasis. The reverse halo sign (atoll sign) is considered to be highly specific, although only seen in 20% of patients with COP. It is characterized by central ground-glass opacity surrounded by a ring or partial ring of consolidation. In addition to these typical CT features, other less specific findings can be encountered, such as irregular linear opacities, solitary focal lesions, and multiple nodules (Akira et al. 1998).

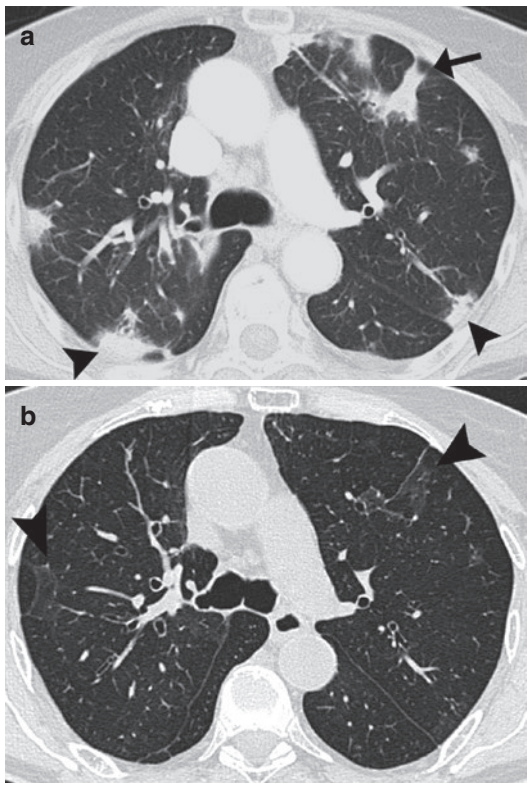

Fig. 10 Axial CT image in a 75-year-old woman with COP shows bilateral, peripherally located patchy lung consolidation (*arrowheads*). In one of the lesions, the subpleural space is typically spared (*arrow*) (**a**). Follow-up CT image obtained after 4 weeks of corticosteroid therapy shows subtotal resolution of the lung abnormalities with residual ground-glass opacities (*arrowheads*) (**b**)

4.1.4 Respiratory Bronchiolitis-Associated Interstitial Lung Disease (RB-ILD)

RB-ILD is exclusively encountered in smokers and is thought to represent a symptomatic variant of the histologically common and incidental finding of respiratory bronchiolitis (RB). Patients are usually 30–50 years old and men are affected nearly twice as often as women. After smoking cessation, prognosis is excellent. Histologically, RB-ILD is characterized by pigmented alveolar macrophages within the bronchioles. The typical HRCT features of RB-ILD are centrilobular nodules ("airspace nodules," small nodules with ground-glass opacity) that are randomly distributed or have upper lobe predominance (Heyneman et al. 1999) (Fig. 11a). Additional CT features are diffuse ground-glass opacities, bronchial wall thickening, and coexisting centrilobular emphysema (Fig. 11b).

4.1.5 Desquamative Interstitial Pneumonia (DIP)

DIP is strongly associated with cigarette smoking and is considered to represent the end of a spectrum of RB-ILD. There is a male predominance and patients usually present between 30–50 years of age. Most patients improve with smoking cessation and corticosteroid therapy. Histologically, DIP shows diffuse involvement, with filling of alveolar spaces with macrophages and desquamated alveolar cells, compared to the bronchiolocentric involvement in RB-ILD. On HRCT, DIP is characterized by extensive and diffuse ground-glass opacities with peripheral and lower lobe predominance (Akira et al. 1997) (Fig. 12). The presence of small cystic spaces and irregular linear opacities are indicative of fibrotic changes.

4.1.6 Lymphoid Interstitial Pneumonia (LIP)

LIP rarely occurs as an idiopathic disease. It is usually seen in conjunction with systemic disorders, most notably human immunodeficiency virus (HIV) infection, Sjögren syndrome, and variable immunodeficiency syndromes (Swigris et al. 2002). LIP is more common in women than in men, and typically, patients become symptomatic in the fifth decade of life. Histologically, LIP

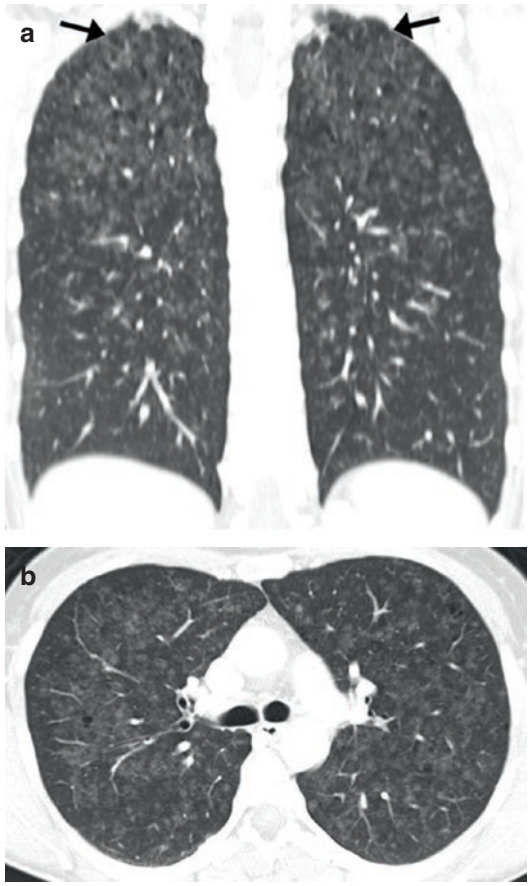

Fig. 11 (**a**, **b**) RB-ILD in a 44-year-old female cigarette smoker. Coronal CT image shows scattered, poorly defined centrilobular nodules that are predominantly located in the upper lung lobes. Note mild coexisting centrilobular emphysema (*arrows*). (**b**) Axial CT image shows centrilobular nodules, patchy ground-glass opacities, and discrete zentrilobular emphysema

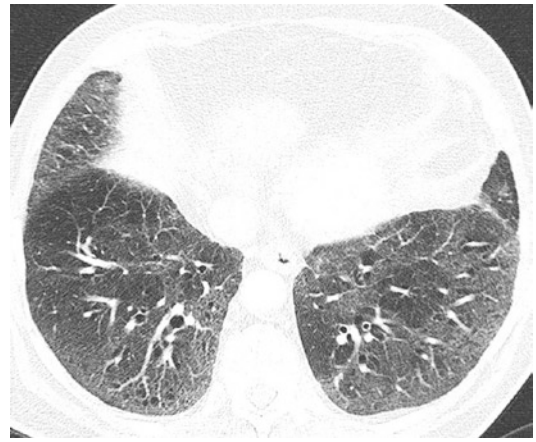

Fig. 12 Desquamative interstitial pneumonia (DIP). HRCT shows bilateral, patchy peripheral ground-glass opacities with a subpleural predominance and coexisting mild bronchial wall thickening. In the right lower lobe, small cystic lucencies are present

Fig. 13 Lymphoid interstitial pneumonia (LIP) in a 48-year-old woman with crazy paving pattern. Axial CT image shows extensive ground-glass opacities and interlobular septal thickening. Scattered thin-walled cysts are also present

is characterized by diffuse interstitial cellular infiltrates that are composed of lymphocytes, plasma cells, and histiocytes. While the interstitium is expanded by these infiltrates, the alveolar airspaces are partially collapsed. The HRCT findings of LIP consist of bilateral, diffuse, or patchy ground-glass opacities, poorly defined centrilobular nodules, and cystic airspaces. The combination of diffuse ground-glass opacities and thickening of the interlobular septa results in the crazy paving pattern (Fig. 13). The mechanism of cyst formation has been postulated to be secondary to partial bronchiolar obstruction with air trapping due to peribronchiolar lymphocytic infiltration (Desai et al. 1997).

4.1.7 Acute Interstitial Pneumonia (AIP)

AIP differs from the other IIPs in its acute course of disease, with rapid onset of dyspnea and cough, followed by respiratory failure and a high acute mortality rate of 50% or more (American Thoracic Society/European Respiratory Society 2002). AIP was formerly referred to as "Hamman-Rich syndrome." The histological and radiological features of AIP are similar to those of acute respiratory distress syndrome (ARDS) and can be subdivided

into an acute or exudative phase and a late or organizing phase. CT obtained in the early phase shows extensive ground-glass opacities, sometimes in a geographic distribution (Fig. 14a). In addition, areas of consolidation can be observed in the dependent areas of the lungs. In patients who survive the acute phase of disease, CT shows fibrotic changes with architectural distortion and traction bronchiectasis, predominantly in the nondependent areas of the lung (Fig. 14b).

4.2 Sarcoidosis

Sarcoidosis is a common systemic disorder of unknown cause characterized by the presence of noncaseating granulomas, which either can dissolve or cause fibrosis. Almost any organ can be affected, but the lungs are most frequently involved.

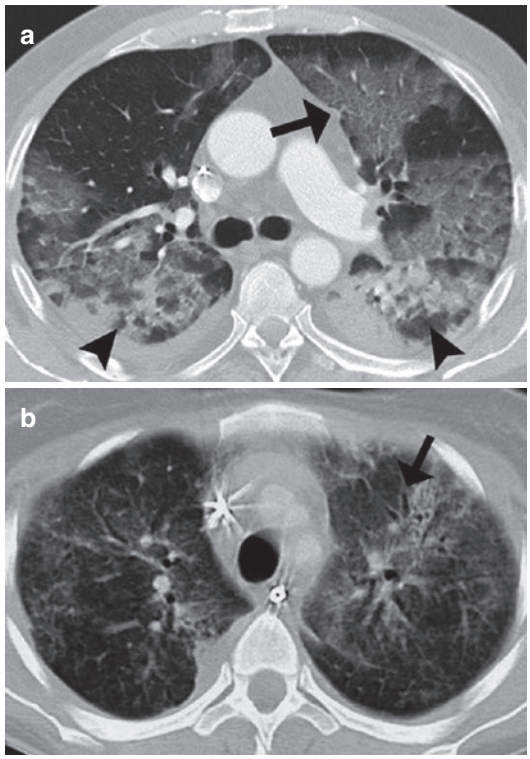

Fig. 14 (**a**, **b**) Acute interstitial pneumonia (AIP) in a 58-year-old patient. Axial CT image shows bilateral ground-glass opacities in a geographic distribution (*arrow*). Consolidation is seen in the more dependent lung (*arrowheads*). Small coexisting bilateral pleural effusions are present (**a**). Fibrotic changes with traction bronchiectasis (*arrow*) and architectural distortion in the late phase of acute AIP (**b**)

The mean age of patients is between 20 and 40 years and there is a slight female predominance (1999). In up to 50% of patients, sarcoidosis is incidentally discovered on radiographs. Common clinical symptoms include respiratory illness, skin lesions, fatigue, and weight loss. Lofgren's syndrome is a classic clinical presentation with fever, erythema nodosum, arthralgias, bihilar lymphadenopathy, and a usually benign course of disease.

The diagnosis is established on the basis of clinical and radiological findings, supported by histology from transbronchial biopsy. Spontaneous remissions occur in nearly two-thirds of patients, but the course is chronic or progressive in 10–30% (Costabel and Hunninghake 1999). The appropriate treatment depends on clinical and imaging findings and is based on corticosteroids. In patients with end-stage sarcoidosis lung transplantation has been successfully performed, but is associated with high recurrence rates of sarcoidosis (35%) (Collins et al. 2001).

For the staging of sarcoidosis a system based on chest radiographs is in clinical use; stage I consists of bilateral hilar adenopathy; in stage II sarcoidosis, patients have bilateral hilar adenopathy and diffuse parenchymal infiltration; stage III describes parenchymal infiltration without hilar adenopathy. Some authorities use a stage IV classification to indicate irreversible fibrosis.

In patients with sarcoidosis, CT scans of the lung are included routinely in the diagnostic workup at initial evaluation and at follow-up. Specifically, they are indicated in the setting of atypical clinical and/or chest radiograph findings, for the detection of complications of the lung disease (e.g., pulmonary fibrosis, superimposed infection, malignancy), and when chest radiographs are normal, despite clinical suspicion of the disease (Costabel and Hunninghake 1999).

The chest can be involved in sarcoidosis in many ways, and because of the multitude of

Fig. 15 27-year-old woman with chronic sarcoidosis. Coronal CT image displays extensive mediastinal lymphadenopathy. Lymph nodes show punctuates calcifications.

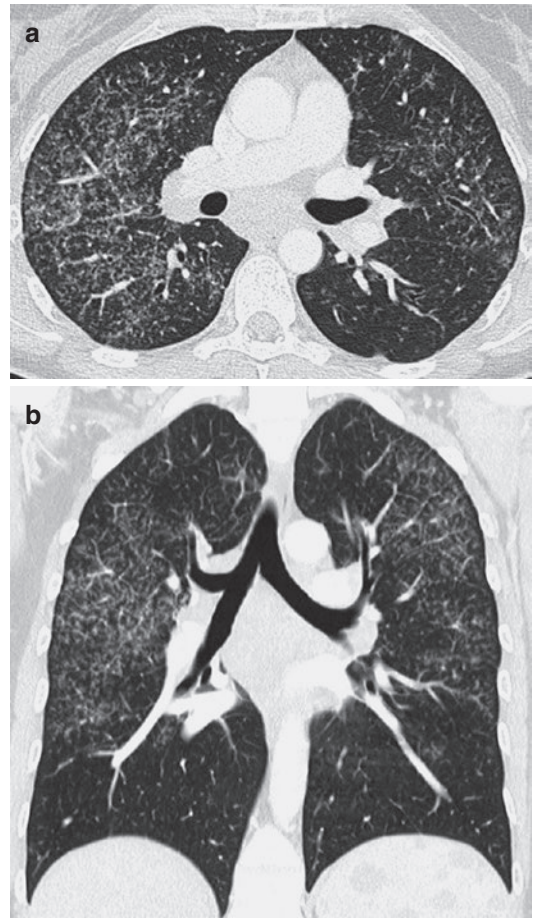

Fig. 16 31-year-old woman with sarcoidosis. (**a**) Axial CT image shows multiple uniformly sized nodules as well as nodular thickening of the interlobular septa and the bronchial walls. (**b**) The upper lobe predominance of the nodules can be seen on the coronal CT image

potentially different findings, sarcoidosis can be regarded as one of the great "mimickers" in thoracic radiology. The most common intrathoracic manifestation of sarcoidosis is the presence of mediastinal lymphadenopathy with usually bilateral and rather symmetric involvement of hilar lymph nodes. They can calcify in chronic disease and then show amorphous, punctate, or eggshell calcifications (Fig. 15). In patients with sarcoidosis and parenchymal involvement nodular opacities are the predominant finding. These nodules typically range in size between 1 and 5 mm and are usually well defined. They have a perilymphatic distribution, and thus preferentially lie adjacent to the fissures and interlobular septa, along pleural surfaces, and along central peribronchovascular structures (Fig. 16). There is a predilection for the upper lobes and the superior segments of the lower lobes of both lungs.

Sarcoid nodules sometimes tend to coalesce and form large parenchmyal nodules with surrounding loosely aggregated small nodules. As the shape of these coalescent granulomas resembles a galaxy, it is referred to as the sarcoid "galaxy sign" (Nakatsu et al. 2002) (Fig. 17). Occasionally, a single large nodule may be present in sarcoidosis and resemble bronchogenic carcinoma. Ground-glass opacities are common in sarcoidosis and have been postulated to represent alveolitis in early reports; however, according to pathologic correlation ground-glass opacities in sarcoidosis are more likely to represent microgranulomas with or without perigranulomatous fibrosis (Nishimura et al. 1993). Patients with predominant ground-glass opacities on initial CT scan have a worse prognosis than patients with a predominant nodular pattern (Murdoch and Muller 1992; Akira et al. 2005).

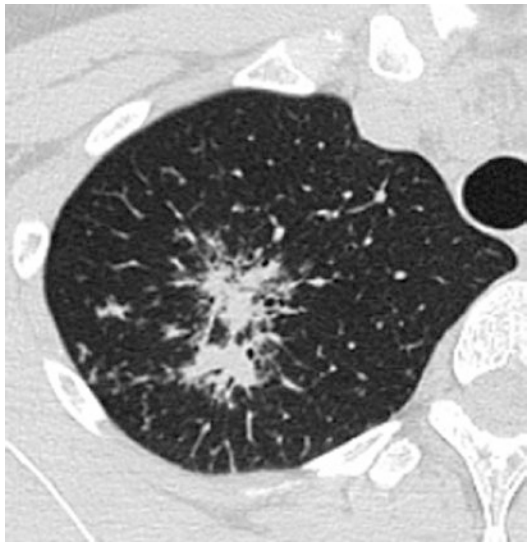

Fig. 17 41-year-old man with sarcoidosis. The parenchymal nodules in the right upper lobe tend to coalesce and form a large parenchymal nodule surrounded by loosely aggregated small nodules. As this resembles a galaxy it is referred to as the "sarcoid galaxy sign"

When sarcoidosis progresses to fibrosis, architectural distortion and traction bronchiectasis classically radiating from the hilum to the adjacent upper and lower lobes can be found. Other common CT abnormalities in fibrotic sarcoidosis include honeycombing, cysts, and bulla formation. Airway stenosis in sarcoidosis is usually due to extrinsic scarring, or to endobronchial granulomas, whereas lymphadenopathy alone is a rare cause of symptomatic airway narrowing.

Pneumoconiosis may simulate the appearance of sarcoidosis, but is usually easily diagnosed when correlated with clinical history.

Lymphangiosis carcinomatosa usually occurs in patients with a known history of malignancy and patients tend to be older than patients with sarcoidosis. Also lymphangiosis carcinomatosa may be unilateral whereas sarcoidosis is typically bilateral, symmetric and upper lobe predominant.

Primary tuberculosis, lymphoma, and mediastinal metastases from other tumors usually present with asymmetrical nodal enlargement as opposed to the bihilar, and often symmetric hilar lymphadenopathy in stage I sarcoidosis.

4.3 Miscellaneous Rare Forms of Interstitial Lung Disease of Unknown Etiology

4.3.1 Pulmonary Langerhans Cell Histiocytosis

Pulmonary Langerhans cell histiocytosis (PLCH) (formerly called histiocytosis X) is a rare interstitial lung disease of unknown cause that primarily affects cigarette smokers under 40 years of age. Most patients present with cough and dyspnea; sometimes additional systemic symptoms, such as fatigue, weight loss, and fever, are reported. Smoking cessation is the most important component in the therapeutic management of PLCH, with stabilization or regression of clinical and radiographic features in the majority of patients. CT is very sensitive for the detection of PLCH and a correct diagnosis can be achieved in over 80% of cases (Grenier et al. 1991). On CT, PLCH is characterized by a combination of small nodules (1–10 mm) and cysts. The cysts are thought to arise by cavitation of the nodules, have a variable wall thickness, and are often irregularly outlined (Abbott et al. 2004) (Fig. 18a). Usually, the lung abnormalities are most prominent in the upper lobes, with relative sparing of the lung bases near the costophrenic sulci (Fig. 18b). In later phases of the disease, nodules are less obvious and cysts are the predominant feature. In this setting, PLCH may mimic lymphangioleiomyomatosis, but the latter occurs almost exclusively in women, affects the lung diffusively without sparing of the lung bases, and is characterized by uniformly sized cysts.

4.3.2 Lymphangioleiomyomatosis

Lymphangioleiomyomatosis (LAM) is a rare interstitial lung disease that affects women of childbearing age exclusively. The tuberous sclerosis complex (TSC), an autosomal dominant inherited disorder, is associated with parenchymal lung changes identical to LAM (Pallisa et al. 2002).

Histologically, LAM is characterized by an abnormal proliferation of smooth muscle cells (LAM cells) in the lungs and in the thoracic and retroperitoneal lymphatics. The most common

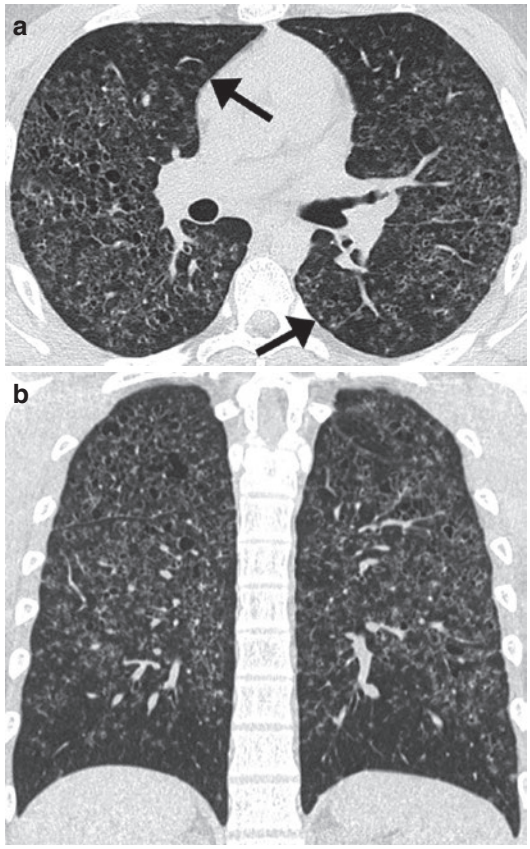

Fig. 18 (**a**, **b**) Pulmonary Langerhans cell histiocytosis in a 26-year-old man. Axial CT image demonstrates bilateral, thin-walled cysts of variable size and multiple, ill-defined nodules (*arrows*) (**a**). Coronal CT image better demonstrates the upper and middle lung zone predominance with relative sparing of the lung bases (**b**)

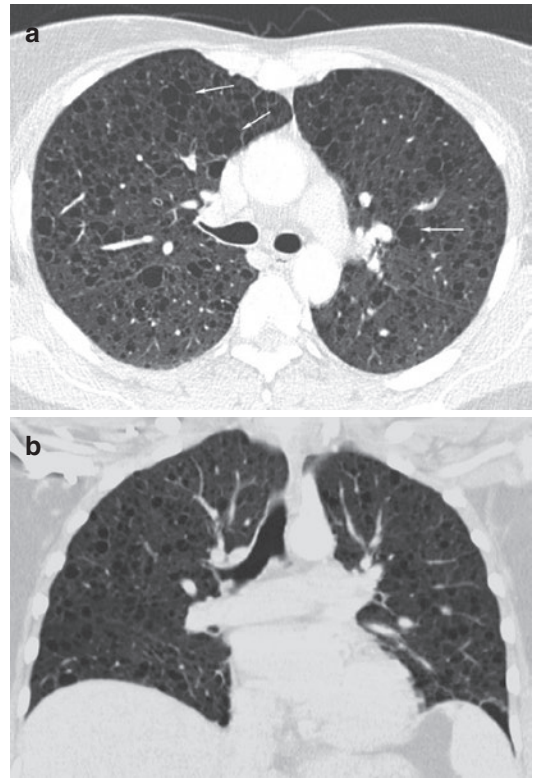

Fig. 19 (**a**, **b**) 30-year-old woman with tuberous sclerosis complex. Axial CT image shows multiple thin-walled cysts in a uniform distribution. The cysts adjacent to the upper right mediastinum tend to conflate (*white arrows*) (**a**). Coronal CT image displays the uniform and bilateral distribution of the cysts throughout both lungs. The lung parenchyma between the cysts is inconspicuous (**b**)

initial presenting symptoms are dyspnea, spontaneous pneumothorax, and cough (Johnson 1999). The clinical course of LAM is variable. Normally, the disease progresses slowly with continuous deterioration of pulmonary function. Ultimately, it leads to respiratory failure. Because LAM deteriorates with pregnancy and the use of exogeneous estrogen, several attempts at anti-estrogen therapies have been made with controversial results (Taylor et al. 1990). Lung transplantation is indicated in patients with end-stage disease. Apart from the common postoperative complications of transplantation, recurrent disease in the donor lung can occur.

The key findings on CT are uniformly distributed, thin-walled cysts that tend to confluate (Fig. 19). The cysts can be up to 3 cm in diameter and are equally and symmetrically distributed throughout both lungs. Usually, the cyst shape is round; however, in some cases, they can be of ovoid, polygonal, or irregular shape. Cyst wall thickness ranges from barely susceptible to up to 2 mm. On expiratory scans, cyst size decreases, suggesting a communication with the airway system. The lung parenchyma in between the cysts is usually inconspicuous, but, in the highly cellular forms of LAM, small nodules, reticular opacification, and ground-glass attenuation can be found (Aberle et al. 1990). Pneumothorax is common in LAM, and occurs in about 80% of patients within the course of the disease. About 8–14% of patients develop pulmonary hemorrhage, which presents as ground-glass opacity on HRCT (Lenoir et al. 1990). Pleural chylous effusions can be found in up to 14% of patients, and are indistinguishable from protein-rich effusions of other origin on

CT. In addition, dilatation of the thoracic duct, as well as mediastinal, hilar, and retrocrural adenopathy, can be found in patients with LAM.

In more than 70% of patients with LAM, renal angiomyolipomas can be found, which show a characteristic appearance, with negative CT values due to their fat content. In some cases, retroperitoneal cystic hypoattenuating masses indicative of lymphangioleiomyomas can be found. Chylous ascites and lymphadenopathy are further extrathoracic findings in some patients (Pallisa et al. 2002).

The most important differential diagnoses for LAM are Langerhans cell histiocytosis, and panlobular emphysema. In contrast to LAM, in Langerhans cell histiocytosis, the costophrenic sulci are usually spared, the cysts can be thick-walled and irregularly outlined, and nodules are predominant in the early stage of disease (Bonelli et al. 1998). Panlobular emphysema is associated with alpha-1-antiprotease deficiency. The most distinct feature of emphysema is the absence of defined walls in the areas of low attenuation, whereas cysts in LAM almost invariably present with walls (Johnson 1999).

4.3.3 Eosinophilic Pneumonia

Eosinophilic pneumonia is divided into acute eosinophilic pneumonia (AEP) and chronic eosinophilic pneumonia (CEP). The pathogenesis of both forms is still unknown, but it is speculated to be a hypersensitivity reaction to an unknown antigen. However, AEP has been reported after cigarette smoking, dust exposure, and smoke from fireworks. The mean age of patients with CEP is 40; AEP occurs at all ages. AEP shows no gender predominance, whereas CEP occurs more often in women. Histologically, diffuse alveolar damage associated with interstitial and alveolar eosinophilia is found in AEP (Tazelaar et al. 1997); in CEP, an accumulation of eosinophils and lymphocytes in the interstitium and alveoli, and sometimes interstitial fibrosis, is found.

AEP clinically presents as an acute febrile illness with dyspnea, pleuritic chest pain, myalgias, and respiratory failure. In AEP, blood eosinophilia is often absent, but more than 25% eosinophils are found in the bronchial lavage fluid of these patients. CEP has an insidious onset with fever, malaise, weight loss, and dyspnea. About 90% of these patients suffer from asthmatic symptoms. In CEP, peripheral blood eosinophilia is present in more than 90% of cases, and there is an increased number of eosinophils in the bronchial lavage fluid as well (Allen and Davis 1994). Both AEP and CEP are often misdiagnosed as pneumonia, which can delay the correct diagnosis. Both AEP and CEP show a rapid response to corticosteroids, and there usually is rapid clearing of clinical and radiographic abnormalities within several days (Allen and Davis 1994).

At CT, AEP shows bilateral peripheral ground-glass opacities, with lower lobe predominance (Fig. 20). In addition, interlobar septal thickening and thickening of the bronchovascular bundles,

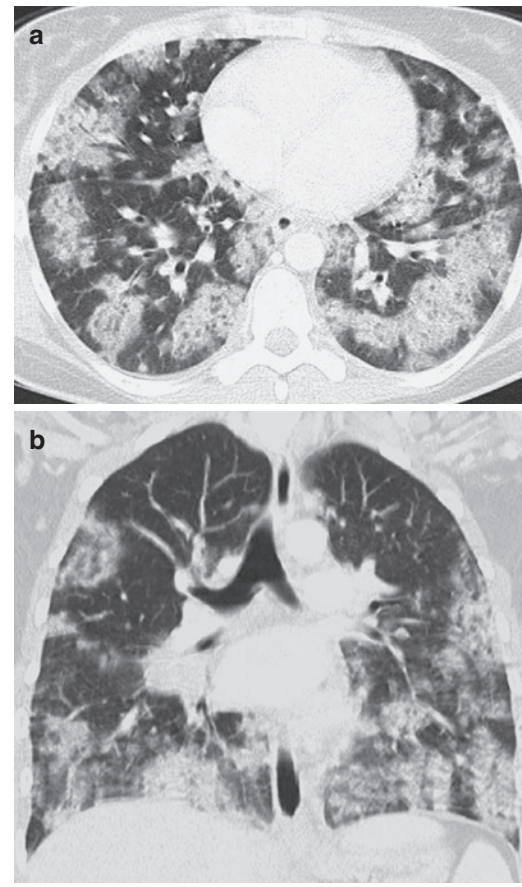

Fig. 20 (**a**, **b**) Acute eosinophilic pneumonia in a 37-year-old female with BAL fluid eosinophilia. Axial CT image obtained 5 days after onset of dyspnea shows peripherally distributed patchy areas of consolidation and ground-glass opacities accompanied by interlobular septal thickening (**a**). Coronal CT image displays the lower lobe predominance of the infiltrates (**b**)

as well as localized areas of consolidation, can be seen. AEP is very commonly associated with pleural effusions (Allen and Davis 1994; Johkoh et al. 2000). The HRCT findings of AEP are nonspecific and may be indistinguishable from pulmonary edema, acute respiratory distress syndrome, atypical pneumonia, and hemorrhage.

CEP shows upper lobe predominance and peripheral nonsegmental consolidations (Fig. 21). Consolidations can persist for some time, but, in the absence of treatment, they tend to migrate. Consolidations are often accompanied by ground-glass opacities, and a "crazy paving" appearance of the consolidations can also be seen in many cases. Pleural effusions are rare in CEP (Mayo et al. 1989; Johkoh et al. 2000). The HRCT findings of CEP are very similar to those of organizing pneumonia, both presenting with peripheral, nonsegmental consolidation. However, CEP has an upper lobe predominance, whereas organizing pneumonia predominantly involves the lower lobes.

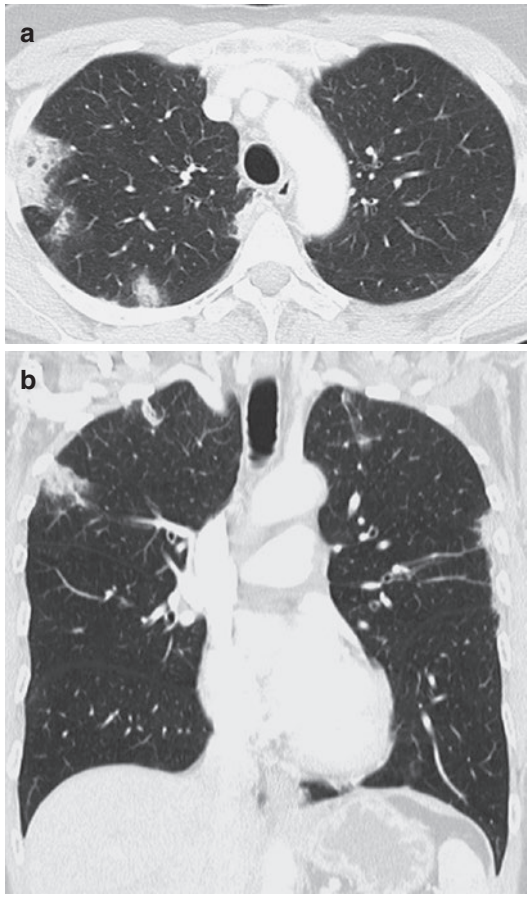

Fig. 21 (**a**, **b**) Chronic eosinophilic pneumonia in a 56-year-old man presenting with a 4 week history of cough and fever. Moderate blood eosinophilia is found in laboratory workup. Axial CT image shows strikingly peripheral wedge shaped airspace consolidations (**a**). The upper lobe predominance of the consolidations is displayed on coronal CT image (**b**)

4.3.4 Pulmonary Alveolar Proteinosis

Pulmonary alveolar proteinosis (PAP) is a rare interstitial lung disease with an incidence of 3.7 per million. It is characterized by filling of the alveoli with a lipid-rich proteinaceous material (Rosen et al. 1958). Three different forms of PAP can be distinguished: an autosomal recessive congenital form (2%); a secondary form (10%) that is associated with various conditions, such as hematopoietic disorders (especially myelogenous leukemias), silicosis, immunodeficiency disorders, malignancies, and some infections; and an idiopathic form (90%). In Idiopathic PAP, several mechanisms are responsible for phospholipid accumulation in the alveoli. Whether this accumulation is caused by reduced clearance or overproduction is not yet clear (Prakash et al. 1987). The median age of the patients is about 40 years, and most patients are men and have a history of smoking (Ben-Dov et al. 1999). Patients present with dyspnea or cough. The symptoms are usually out of proportion to the radiological findings (clinical–radiological discrepancy). In 13% of patients with PAP, secondary infections with nocardia, cryptococcus, or mycobacteria are observed. The treatment for PAP is bronchoalveolar lavage with sterile saline, and prognosis is generally good with whole lung lavage.

HRCT is characterized by bilateral, symmetrical, geometric areas of ground-glass attenuation (Fig. 22). The interlobular septa are thickened, and a fine network of intralobular lines can be seen. These changes are responsible for the so-called "crazy paving" pattern. The disease does not have any preferential zonal distribution (Holbert et al. 2001). Architectural distortion and bronchiectasis are absent normally; however, in a small percentage of patients, pulmonary fibrosis can be found. Although the

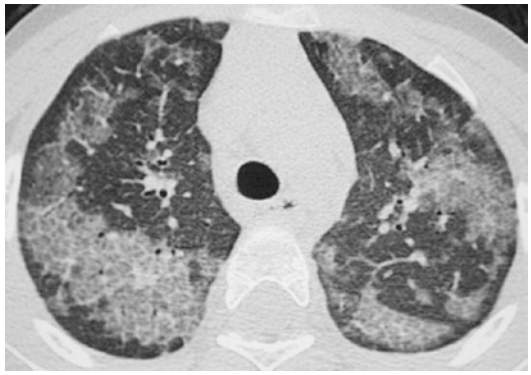

Fig. 22 Alveolar proteinosis (AP) in 40-year-old man with myelogenous leucemia presenting with cough and dyspnea. Axial CT image displays bilateral geographical areas of ground-glass opacity. Interlobular septa are thickened and within these areas a fine reticular network of interlobular lines can be seen. These changes are referred to as the typical "crazy paving" appearance of AP

crazy paving pattern on HRCT is suggestive of PAP, this pattern can also be observed in a number of other interstitial and airspace diseases, such as pulmonary hemorrhage, pulmonary edema, hypersensitivity pneumonitis, and pulmonary adenocarcinoma (previously termed bronchioloalveolar carcinoma). The diagnosis is made by bronchoalveolar lavage and typical clinical findings. Nevertheless, the gold standard in diagnosis remains open lung biopsy.

4.3.5 Pulmonary Microlithiasis

Pulmonary alveolar mircrolithiasis (PAM) is a rare condition characterized by the formation of intraalveolar microliths (calcospherites). The pathogenesis of the micronodular calcifications is still unknown. In about 50% of cases, pulmonary alveolar microlithiasis occurs as an autosomal recessive hereditary lung disease (Sosman et al. 1957). Most cases of microlithiasis are found in Turkey (Ucan et al. 1993). The disease usually occurs between 30 and 50 years of age and pediatric cases are rare. In hereditary cases, there is slight female predominance.

The disease is typically detected incidentally on chest films obtained for other reasons, and clinical symptoms are disproportional to the extent of radiologic findings. Occasionally, patients present with stress-induced dyspnea, malaise, or fatigue. As PAM progresses with the formation of tiny (0.01–3 mm) microspheres in the alveoli, it can ultimately lead to respiratory failure and cor pulmonale.

In early stages, diffuse ground-glass opacifications are found throughout both lungs on CT. Still, the presence of calcified micronodules is most characteristic. The distribution of the micronodules is miliary, but there is a tendency toward greater involvement of the posterior segments of the lower lobes and the anterior segments of the upper lobes (Fig. 23). Due to the intra and periseptal accumulation of micronodules, interlobular septal thickening is found in almost all patients. In addition, subpleural septal thickening is frequently detected.

As the disease progresses, subpleural emphysema and the formation of thin-walled subpleural cysts are pathognomonic findings in PAM and might represent early lung fibrosis. The subpleural cysts are accountable for the black subpleural line on chest X-rays (Korn et al. 1992). The main differential diagnoses include miliary tuberculosis, sarcoidosis, metastatic pulmonary calcification associated with hemodialysis, silicosis, and pulmonary hemosiderosis.

Usually, the disease progresses very slowly, but can result in cardiac and pulmonary failure. There is no known treatment, except lung transplantation in end-stage disease.

Fig. 23 37-year-old man with pulmonary alveolar microlithiasis. Axial CT image shows miliary distributed calcified micronodules predominantly located in the middle and lower zones of both lungs. Also note the formation of small subpleural cysts and subpleural emphysema and the formation of the pathognomonic *black* subpleural line (*white arrows*)

5 Interstitial Lung Diseases of Known Cause

5.1 Occupational and Environmental Lung Disease

Occupational and environmental lung disease comprises a wide spectrum of lung disorders caused by the inhalation or ingestion of organic and inorganic particles and chemicals. CT is very sensitive in depicting the parenchymal, as well as airway and pleural abnormalities that are associated with these diseases.

5.1.1 Hypersensitivity Pneumonitis

Hypersensitivity pneumonitis (HP), also known as exogenous allergic alveolitis (EEA), is an immunologic lung disease caused by repeated exposure and sensitization to various organic and chemical antigens that lead to diffuse inflammation of the lung parenchyma. The most common diseases are farmer's lung and bird fancier's lung due to aspergillus antigen and avian proteins, respectively. Based on the length and intensity of exposure and subsequent duration of illness, clinical presentations of HP are categorized as acute, subacute, and chronic progressive. In acute HP, patients present 4–12 h following heavy exposure to an inciting agent with fever, chills, and myalgias. In subacute and chronic HP, patients have an insidious onset of cough, progressive dyspnea, fatigue, and weight loss. HRCT in acute HP typically shows diffuse ground-glass opacities and centrilobular nodules, most commonly in a random distribution (Tomiyama et al. 2000). However, due to the short duration of symptoms patients rarely undergo CT scanning in the acute phase. In the subacute phase, centrilobular nodules become more prominent and patchy ground-glass opacities can be found. In some patients cystic lesions (3–25 mm) have been observed (Franquet et al. 2003). Chronic HP is characterized by the presence of reticulation due to fibrosis superimposed on findings of subacute HP (Fig. 24). The abnormalities are usually predominantly located in the upper lobes, while the lung bases are relatively spared (Silva et al. 2008). Other common findings in chronic HP include a mosaic attenuation pattern and air trapping on expiratory imaging (Small et al. 1996).

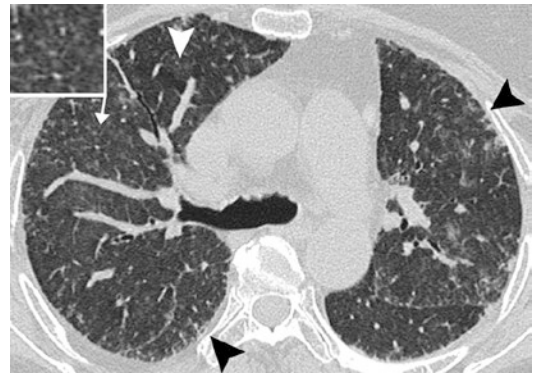

Fig. 24 Chronic hypersensitivity pneumonitis in a 52-year-old man related to mold exposure. Axial CT image shows patchy ground-glass opacities with associated centrilobular nodules (inset: magnified view of centrilobular nodules). Also note mild subpleural reticular opacities (*black arrowheads*) indicating fibrosis, and subtle mosaic attenuation (*white arrowhead*)

5.1.2 Pneumoconiosis

Pneumoconiosis is a non-neoplastic reaction to the inhalation and accumulation of dust particles in the lung. The particles are engulfed by alveolar macrophages that release inflammatory cytokines and induce fibrotic changes. The classification of pneumoconiosis is based on chest radiographs using the International Labor Organization (ILO) classification scheme. The HRCT features in patients with silicosis and coal worker pneumoconiosis consist of small, well-circumscribed nodules that are usually 2–5 mm in diameter and predominantly affect the upper and posterior lung zones. The nodules have a perilymphatic distribution, thus affecting the interlobular septa and the peribronchovsacular and subpleural interstitium. The nodules in silicosis tend to be larger and better defined than those in coal worker pneumoconiosis (Kim et al. 2001). Occasionally, eggshell calcifications in the hilar and mediastinal lymph nodes are seen. The presence of nodules larger than 1 cm is indicative of complicated pneumoconiosis, also known as progressive massive fibrosis. These nodules coalesce and form conglomerate masses that are typically located in the upper lobe of the lung. In large lesions, cavitation may occur, which is due to either ischemic

necrosis or superinfection. In advanced disease, hilar retraction and compensatory emphysema, particularly in the lower lobes, is seen (Fig. 25).

The parenchymal lung manifestations related to asbestos exposure are referred to as asbestosis and differ from the previously described "classic" pneumoconiosis. Early asbestosis is characterized by subpleural linear and reticular opacities that are predominantly located in the posterior lung bases. To distinguish these abnormalities from gravity-related physiologic changes, prone scans should be included in cases of suspected asbestosis. Other typical findings in asbestosis include thickened interlobular septa and centrilobular nodules. In advanced disease, CT shows bands of fibrosis, traction bronchiectasis, and honeycombing. In addition, other asbestos-related lung abnormalities, such as pleural effusion, pleural plaques, and round atelectasis can be found.

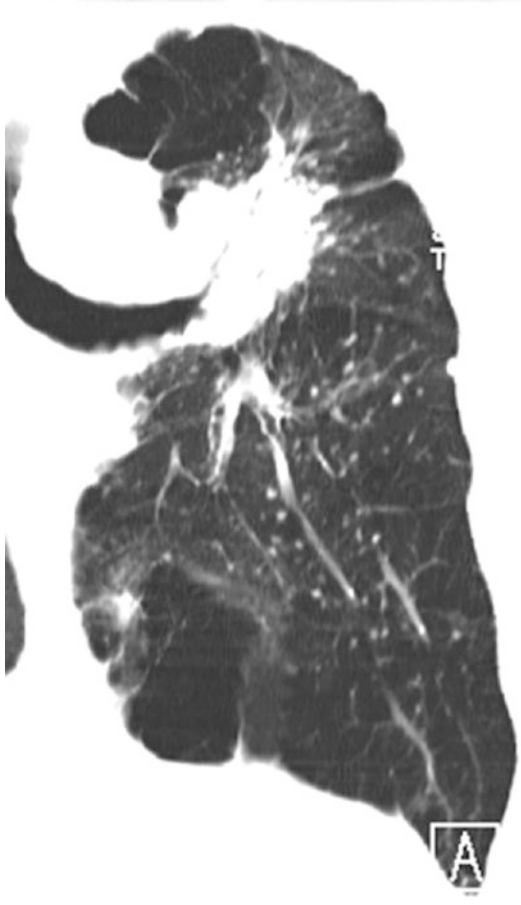

Fig. 25 Silicosis with progressive massive fibrosis in a 72-year-old man. Coronal CT image shows a large perihilar mass in the left upper lobe. There is retraction of the hilus and marked emphysema. In addition, some scattered small nodules are present

5.1.3 Drug-Induced Lung Disease

Drug-induced lung injury is a common cause of acute and chronic lung disease, and most commonly occurs with cytotoxic agents, such as bleomycin, busulfan, carmustine, and cyclophosphamide (Ellis et al. 2000). The most common patterns of drug-induced lung disease include: pulmonary edema and hemorrhage; diffuse alveolar damage (DAD)/acute respiratory distress syndrome (ARDS); organizing pneumonia (OP); nonspecific interstitial pneumonia (NSIP), usual interstitial pneumonia (UIP); hypersensitivity pneumonitis; and eosinophilic pneumonia. In early drug-induced DAD (1st week after lung injury), CT shows diffuse ground-glass opacities and consolidations, whereas, in the late phase of disease (after 1 or 2 weeks), fibrotic changes occur, such as irregular linear opacities, architectural distortion, and traction bronchiectasis. The HRCT manifestations of NSIP consist of scattered ground-glass opacities and irregular linear opacities (Fig. 26). The sparing of the outermost subpleural lung is highly suggestive of NSIP. HRCT findings in UIP include reticular opacities, traction bronchiectasis and honeycombing. Drug-induced OP is identical to cryptogenic organizing pneumonia (COP), and manifests on CT with bilateral areas of ground-glass opacities or consolidations that are often peripheral in distribution. Hypersensitivity pneumonitis usually becomes clinically apparent within hours or days after institution of drug therapy and HRCT findings are similar to those caused by inhalational agents (Rossi et al. 2000) with ground-glass opacities, centrilobular nodules, mosaic pattern and air trapping and Pulmonary involvement can result in either acute or chronic eosinophilic pneumonia (EP). Drug toxicity is a common cause of eosinophilic pneumonia and is characterized by combined lung abnormality and increased serum or tissue eosinophils. HRCT in EP shows consolidation that are typically distributed peripherally and in the upper lobe. EP usually responds well to cessation of the administered drug and is exceedingly

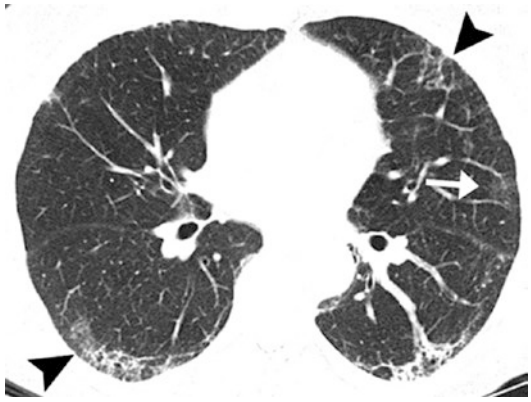

Fig. 26 50-year-old woman with interstitial pneumonia (IP)/nonspecific interstitial pneumonia (NSIP) following bleomycin chemotherapy for Hodgkin's lymphoma. Axial CT image shows irregular linear and reticular opacities (*arrowheads*) with subtle ground-glass opacities (*arrow*) in subpleural distribution

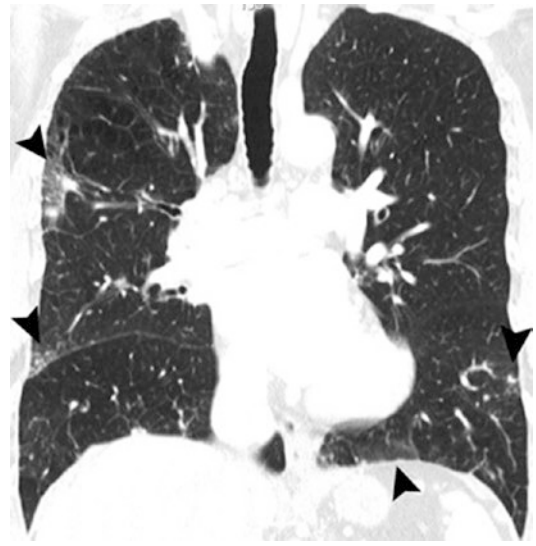

Fig. 27 63-year-old man with organizing pneumonia (OP). The patient was receiving amiodarone for cardiac arrhythmia. Coronal CT image shows bilateral areas of ground-glass opacities in subpleural distribution (*arrowheads*)

sensitive to corticosteroid therapy. Within the group of noncytotoxic drugs, methotrexate and amiodarone frequently cause drug-induced lung diseases in 5–10% of patients. The most common lung injury associated with both drugs is nonspecific interstitial pneumonia. Organizing pneumonia is less commonly associated with noncytotoxic drugs (Fig. 27).

5.2 Radiation-Induced Lung Injury

Radiation-induced lung injury is subdivided clinically and radiologically into an early stage, characterized by acute radiation pneumonitis, and a late stage, characterized by chronic radiation fibrosis. The degree of radiation damage to normal tissue depends particularly on total dose and the fraction of that dose, irradiated volume, individual susceptibility, preexisting lung disease, and previous or concomitant therapy. Early radiation pneumonitis usually develops 1–3 months after the therapy, and the radiographic findings are typically confined to the field of radiation, resulting in a geometric shape of pulmonary opacities with a sharp demarcation line at noninvolved lung areas and disregard of anatomic boundaries. The earliest CT findings consist of subtle ground-glass opacities (Fig. 28).

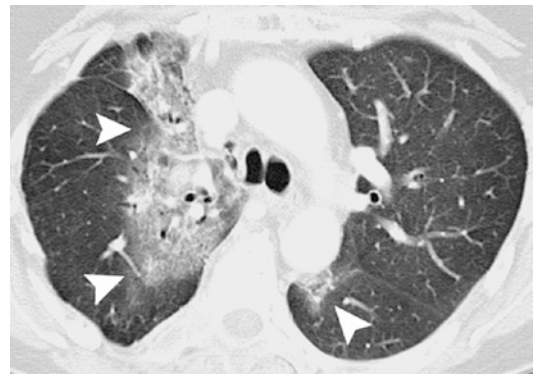

Fig. 28 Acute radiation pneumonitis after treatment of lung cancer. Axial CT image obtained at 4 months after completion of treatment shows paramediastinal ground-glass opacities with sharp lateral margins (*arrowheads*)

These hazy abnormalities can progress to patchy consolidations that sometimes also involve lung areas outside the field of radiation (Davis et al. 1992). Chronic radiation fibrosis evolves within 6–24 months after radiation therapy and develops continuously from the phase of acute pneumonitis. At CT, it is characterized by the presence of reticular opacities, architectural distortion, traction bronchiectasis, and volume loss. The major differential diagnoses in radiation pneumonitis include infection, lymphangitic

carcinomatosis, and recurrence of the original malignancy. Microbial infectious pneumonia is not usually confined to the field of irradiation and runs a more symptomatic clinical course than radiation pneumonitis. In lymphangitic carcinomatosis, the rapid worsening of radiographic abnormalities, with development of irregular, often nodular thickening of the interlobular septa and the bronchovascular bundles, pleural effusions, and diffuse spread to the lung, are the diagnostic clues.

5.3 Collagen Vascular Lung Disease

Lung involvement is common in patients with collagen vascular diseases and may be detected with HRCT before the disease has declared itself or been accurately characterized. Interstitial lung disease is probably most prevalent in systemic sclerosis, but is also a common problem in rheumatoid arthritis (RA), mixed connective tissue disease, dermatomyositis/polymyositis (DMPM), or Sjögren syndrome. Lung involvement less frequently occurs with systemic lupus erythematosus (SLE). The parenchymal manifestations of collagen vascular diseases seen at CT closely resemble those found in idiopathic interstitial pneumonias (IIPs) and can be classified using the same system. Although the proportions of interstitial pneumonias vary, the nonspecific interstitial pneumonia (NSIP) is the most frequently encountered pattern in patients with collagen vascular lung disease, especially in progressive systemic sclerosis (Fig. 29). In keeping with the IIPs, the NSIP pattern is characterized by subpleural reticular opacities and varying proportions of ground-glass opacities, while in patients with UIP, honeycombing and traction-bronchiectasis are the dominant abnormality. The predominance of the NSIP over the UIP pattern might explain the more favorable prognosis in patients with interstitial pneumonia associated with collagen vascular diseases than in those with IIPs (Kim et al. 2002). Organizing pneumonia (OP) is more common in RA than in the other collagen vascular diseases and is

Fig. 29 Axial CT image in a patient with progressive systemic sclerosis shows a mixture of fine reticular and ground-glass opacities (*black arrows*), associated with mild traction bronchiectasis (*white arrow*), consistent with a nonspecific interstitial pneumonia pattern. Note esophageal dilatation (*arrowheads*)

characterized by patchy infiltrates in a peripheral distribution. Lymphoid interstitial pneumonia (LIP) is a typical, but rare complication in Sjögren syndrome in about 1% of patients during the course of their disease (Swigris et al. 2002), and HRCT findings include diffuse or patchy ground-glass opacities and thin-walled perivascular cysts (Fig. 30). In addition to the patterns of interstitial pneumonias, other parenchymal manifestations in collagen vascular diseases include alveolar hemorrhage, especially in patients with SLE, and necrobiotic nodules in patients with RA, which range in size from a few millimeters to a few centimeters (Remy-Jardin et al. 1994), and are usually subpleural in distribution. The increased prevalence of malignant disorders complicating the course of some disorders such as DMPM makes volumetric CT protocols mandatory in the follow-up of these patients.

5.4 Diffuse Pulmonary Hemorrhage

Diffuse bleeding into the alveolar spaces most commonly occurs with immunological and hematological disorders and is clinically characterized by hemoptysis and anemia (Albelda et al.

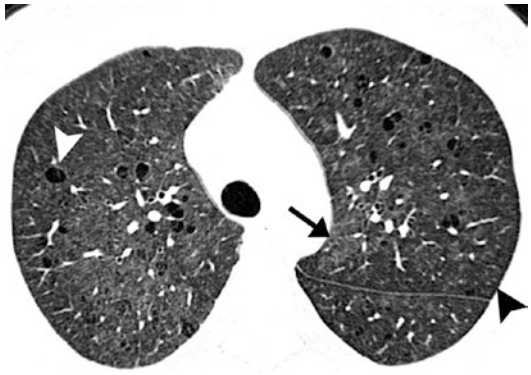

Fig. 30 LIP in a 44-year-old woman with Sjögren syndrome. Axial CT image shows several thin-walled cysts (*white arrowhead*), bilateral patchy ground-glass opacities (*arrow*), and poorly defined centrilobular nodules (*black arrowhead*)

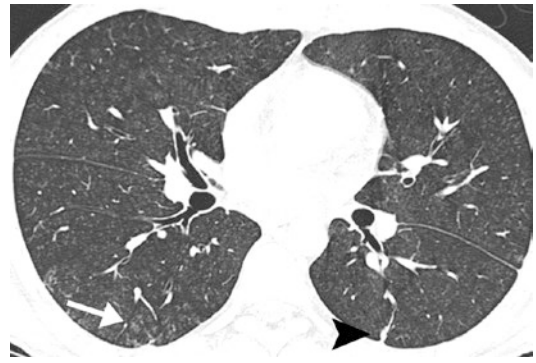

Fig. 31 Goodpasture syndrome in a 21-year-old-man. CT scan shows multiple nodules, subtle ground-glass opacities (*arrow*), and mild interlobular thickening (*arrowhead*)

1985); however, the absence of these symptoms does not rule out the diagnosis of diffuse pulmonary hemorrhage (DPH). DPH must be distinguished from localized pulmonary hemorrhage due to chronic bronchitis, bronchiectasis, malignancy, and infection. DPH can occur in association with many collagen vascular diseases, notably systemic lupus erythematosus (SLE) and vasculitis. Other rare causes of DPH include Goodpasture syndrome and idiopathic pulmonary hemosiderosis. CT is more sensitive than chest radiograph for the detection of pulmonary hemorrhage, and shows diffuse bilateral consolidation or ground-glass opacities in the acute phase (Marasco et al. 1993). In the subacute phase of DPH, multiple small nodules associated with patchy ground-glass opacities and interlobular septal thickening have been observed (Fig. 31). In addition, in patients with granulomatosis with polyangiitis (formerly known as Wegener's granulomatosis), multiple, frequently cavitating nodules and masses, ranging from 5 to 10 cm, can be seen.

References

(1999) Statement on sarcoidosis. Joint Statement of the American Thoracic Society (ATS), the European Respiratory Society (ERS) and the World Association of Sarcoidosis and Other Granulomatous Disorders (WASOG) adopted by the ATS Board of Directors and by the ERS Executive Committee, February 1999. Am J Respir Crit Care Med 160(2):736–755

(2002) American Thoracic Society/European Respiratory Society International Multidisciplinary Consensus Classification of the Idiopathic Interstitial Pneumonias. This joint statement of the American Thoracic Society (ATS), and the European Respiratory Society (ERS) was adopted by the ATS board of directors, June 2001 and by the ERS Executive Committee, June 2001. Am J Respir Crit Care Med 165(2):277–304

Abbott GF, Rosado-de-Christenson ML et al (2004) From the archives of the AFIP: pulmonary Langerhans cell histiocytosis. Radiographics 24(3):821–841

Aberle DR, Hansell DM et al (1990) Lymphangiomyomatosis: CT, chest radiographic, and functional correlations. Radiology 176(2):381–387

Akira M, Yamamoto S et al (1997) Serial computed tomographic evaluation in desquamative interstitial pneumonia. Thorax 52(4):333–337

Akira M, Yamamoto S et al (1998) Bronchiolitis obliterans organizing pneumonia manifesting as multiple large nodules or masses. AJR Am J Roentgenol 170(2):291–295

Akira M, Kozuka T et al (2005) Long-term follow-up CT scan evaluation in patients with pulmonary sarcoidosis. Chest 127(1):185–191

Albelda SM, Gefter WB et al (1985) Diffuse pulmonary hemorrhage: a review and classification. Radiology 154(2):289–297

Allen JN, Davis WB (1994) Eosinophilic lung diseases. Am J Respir Crit Care Med 150(5 Pt 1):1423–1438

Antoniou KM, Wuyts W et al (2016) Medical therapy in idiopathic pulmonary fibrosis. Semin Respir Crit Care Med 37(3):368–377

Ben-Dov I, Kishinevski Y et al (1999) Pulmonary alveolar proteinosis in Israel: ethnic clustering. Isr Med Assoc J 1(2):75–78

Bonelli FS, Hartman TE et al (1998) Accuracy of high-resolution CT in diagnosing lung diseases. AJR Am J Roentgenol 170(6):1507–1512

Bouros D, Hatzakis K et al (2002) Association of malignancy with diseases causing interstitial pulmonary changes. Chest 121(4):1278–1289

Collins J, Hartman MJ et al (2001) Frequency and CT findings of recurrent disease after lung transplantation. Radiology 219(2):503–509

Cordier JF (2000) Organising pneumonia. Thorax 55(4):318–328

Costabel U, Hunninghake GW (1999) ATS/ERS/WASOG statement on sarcoidosis. Sarcoidosis Statement Committee. American Thoracic Society. European Respiratory Society. World Association for Sarcoidosis and Other Granulomatous Disorders. Eur Respir J 14(4):735–737

Davis SD, Yankelevitz DF et al (1992) Radiation effects on the lung: clinical features, pathology, and imaging findings. AJR Am J Roentgenol 159(6):1157–1164

Desai SR, Nicholson AG et al (1997) Benign pulmonary lymphocytic infiltration and amyloidosis: computed tomographic and pathologic features in three cases. J Thorac Imaging 12(3):215–220

Desai SR, Veeraraghavan S et al (2004) CT features of lung disease in patients with systemic sclerosis: comparison with idiopathic pulmonary fibrosis and nonspecific interstitial pneumonia. Radiology 232(2):560–567

Ellis SJ, Cleverley JR et al (2000) Drug-induced lung disease: high-resolution CT findings. AJR Am J Roentgenol 175(4):1019–1024

Franquet T, Hansell DM et al (2003) Lung cysts in subacute hypersensitivity pneumonitis. J Comput Assist Tomogr 27(4):475–478

Gordic S, Morsbach F et al (2014) Ultralow-dose chest computed tomography for pulmonary nodule detection: first performance evaluation of single energy scanning with spectral shaping. Investig Radiol 49(7):465–473

Grenier P, Valeyre D et al (1991) Chronic diffuse interstitial lung disease: diagnostic value of chest radiography and high-resolution CT. Radiology 179(1):123–132

Hansell DM (2001) High-resolution CT of diffuse lung disease: value and limitations. Radiol Clin N Am 39(6):1091–1113

Heyneman LE, Ward S et al (1999) Respiratory bronchiolitis, respiratory bronchiolitis-associated interstitial lung disease, and desquamative interstitial pneumonia: different entities or part of the spectrum of the same disease process? AJR Am J Roentgenol 173(6):1617–1622

Holbert JM, Costello P et al (2001) CT features of pulmonary alveolar proteinosis. AJR Am J Roentgenol 176(5):1287–1294

Johkoh T, Muller NL et al (2000) Eosinophilic lung diseases: diagnostic accuracy of thin-section CT in 111 patients. Radiology 216(3):773–780

Johkoh T, Muller NL et al (2002) Nonspecific interstitial pneumonia: correlation between thin-section CT findings and pathologic subgroups in 55 patients. Radiology 225(1):199–204

JohnsonS(1999)Rarediseases.1.Lymphangioleiomyomatosis: clinical features, management and basic mechanisms. Thorax 54(3):254–264

Katzenstein AL, Myers JL (1998) Idiopathic pulmonary fibrosis: clinical relevance of pathologic classification. Am J Respir Crit Care Med 157(4 Pt 1):1301–1315

Kim KI, Kim CW et al (2001) Imaging of occupational lung disease. Radiographics 21(6):1371–1391

Kim EA, Lee KS et al (2002) Interstitial lung diseases associated with collagen vascular diseases: radiologic and histopathologic findings. Radiographics 22 Spec No:S151–S165

Kim DS, Park JH et al (2006) Acute exacerbation of idiopathic pulmonary fibrosis: frequency and clinical features. Eur Respir J 27(1):143–150

Korn MA, Schurawitzki H et al (1992) Pulmonary alveolar microlithiasis: findings on high-resolution CT. AJR Am J Roentgenol 158(5):981–982

Lee KS, Kullnig P et al (1994) Cryptogenic organizing pneumonia: CT findings in 43 patients. AJR Am J Roentgenol 162(3):543–546

Lenoir S, Grenier P et al (1990) Pulmonary lymphangiomyomatosis and tuberous sclerosis: comparison of radiographic and thin-section CT findings. Radiology 175(2):329–334

Lim HJ, Chung MJ et al (2016) The impact of iterative reconstruction in low-dose computed tomography on the evaluation of diffuse interstitial lung disease. Korean J Radiol 17(6):950–960

Marasco WJ, Fishman EK et al (1993) Acute pulmonary hemorrhage. CT evaluation. Clin Imaging 17(1):77–80

Mayo JR, Webb WR et al (1987) High-resolution CT of the lungs: an optimal approach. Radiology 163(2):507–510

Mayo JR, Muller NL et al (1989) Chronic eosinophilic pneumonia: CT findings in six cases. AJR Am J Roentgenol 153(4):727–730

Mueller-Mang C, Grosse C et al (2007) What every radiologist should know about idiopathic interstitial pneumonias. Radiographics 27(3):595–615

Murata K, Itoh H et al (1986) Centrilobular lesions of the lung: demonstration by high-resolution CT and pathologic correlation. Radiology 161(3):641–645

Murdoch J, Muller NL (1992) Pulmonary sarcoidosis: changes on follow-up CT examination. AJR Am J Roentgenol 159(3):473–477

Nakatsu M, Hatabu H et al (2002) Large coalescent parenchymal nodules in pulmonary sarcoidosis: "sarcoid galaxy" sign. AJR Am J Roentgenol 178(6):1389–1393

Nishimura K, Itoh H et al (1993) Pulmonary sarcoidosis: correlation of CT and histopathologic findings. Radiology 189(1):105–109

Pallisa E, Sanz P et al (2002) Lymphangioleiomyomatosis: pulmonary and abdominal findings with pathologic correlation. Radiographics 22 Spec No:S185–S198

Prakash UB, Barham SS et al (1987) Pulmonary alveolar phospholipoproteinosis: experience with 34 cases and a review. Mayo Clin Proc 62(6):499–518

Prosch H, Schaefer-Prokop CM et al (2013) CT protocols in interstitial lung diseases—a survey among members

of the European Society of Thoracic Imaging and a review of the literature. Eur Radiol 23(6):1553–1563
Raghu G, Collard HR et al (2011) An official ATS/ERS/JRS/ALAT statement: idiopathic pulmonary fibrosis: evidence-based guidelines for diagnosis and management. Am J Respir Crit Care Med 183:788–824
Remy-Jardin M, Remy J et al (1994) Lung changes in rheumatoid arthritis: CT findings. Radiology 193(2):375–382
Rosen SH, Castleman B et al (1958) Pulmonary alveolar proteinosis. N Engl J Med 258(23):1123–1142
Rossi SE, Erasmus JJ et al (2000) Pulmonary drug toxicity: radiologic and pathologic manifestations. Radiographics 20(5):1245–1259
Silva CI, Muller NL et al (2008) Chronic hypersensitivity pneumonitis: differentiation from idiopathic pulmonary fibrosis and nonspecific interstitial pneumonia by using thin-section CT. Radiology 246(1):288–297
Small JH, Flower CD et al (1996) Air-trapping in extrinsic allergic alveolitis on computed tomography. Clin Radiol 51(10):684–688
Sosman MC, Dodd GD et al (1957) The familial occurrence of pulmonary alveolar microlithiasis. Am J Roentgenol Radium Therapy, Nucl Med 77(6):947–1012
Studler U, Gluecker T et al (2005) Image quality from high-resolution CT of the lung: comparison of axial scans and of sections reconstructed from volumetric data acquired using MDCT. AJR Am J Roentgenol 185(3):602–607
Swigris JJ, Berry GJ et al (2002) Lymphoid interstitial pneumonia: a narrative review. Chest 122(6):2150–2164
Taylor JR, Ryu J et al (1990) Lymphangioleiomyomatosis. Clinical course in 32 patients. N Engl J Med 323(18):1254–1260
Tazelaar HD, Linz LJ et al (1997) Acute eosinophilic pneumonia: histopathologic findings in nine patients. Am J Respir Crit Care Med 155(1):296–302
Thabut G, Mal H et al (2003) Survival benefit of lung transplantation for patients with idiopathic pulmonary fibrosis. J Thorac Cardiovasc Surg 126(2):469–475
Tomiyama N, Muller NL et al (2000) Acute parenchymal lung disease in immunocompetent patients: diagnostic accuracy of high-resolution CT. AJR Am J Roentgenol 174(6):1745–1750
Travis WD, Matsui K et al (2000) Idiopathic nonspecific interstitial pneumonia: prognostic significance of cellular and fibrosing patterns: survival comparison with usual interstitial pneumonia and desquamative interstitial pneumonia. Am J Surg Pathol 24(1):19–33
Ucan ES, Keyf AI et al (1993) Pulmonary alveolar microlithiasis: review of Turkish reports. Thorax 48(2):171–173
Webb WR (2006) Thin-section CT of the secondary pulmonary lobule: anatomy and the image—the 2004 Fleischner lecture. Radiology 239(2):322–338
Weibel ER (1979) Fleischner lecture. Looking into the lung: what can it tell us? AJR Am J Roentgenol 133(6):1021–1031